

CLEARED
FOR PUBLIC RELEASE
PL/PA 16 DEC 96

Sensor and Simulation Notes

Note 180

June 1973

Reflection From an Array of Dielectric Posts

R.W. Latham
Northrop Corporate Laboratories
Pasadena, California

Abstract

The reflection of a plane wave incident on a two-dimensional array of infinitely long dielectric posts is investigated. The array is infinite in the direction perpendicular to the propagation vector of the incident wave. This array is considered to be a model of the wooden support structure of the ATLAS simulators. In accordance with this intended application, the maximum post diameter is assumed to be small with respect to both the wavelength of the incident wave and the minimum distance between posts.

The impedance per unit length of a single post is first defined and calculated. Next, the sheet impedance of a single infinite row of identical posts is defined, and determined in terms of the impedance per unit length of the individual posts. The reflection from several rows of posts is then examined. An explicit formula for the reflection coefficient is obtained for the case where each row of the array is modelled as an impedance sheet. The limit where the impedance sheet concept breaks down is pointed out, and a method for extending the simpler results to this more general case is indicated.

PL 96-1980

Sensor and Simulation Notes

Note 180

June 1973

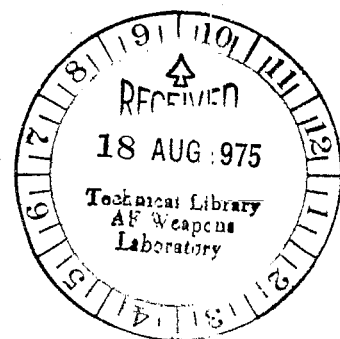
Reflection From an Array of Dielectric Posts

R.W. Latham
Northrop Corporate Laboratories
Pasadena, California

Abstract

The reflection of a plane wave incident on a two-dimensional array of infinitely long dielectric posts is investigated. The array is infinite in the direction perpendicular to the propagation vector of the incident wave. This array is considered to be a model of the wooden support structure of the ATLAS simulators. In accordance with this intended application, the maximum post diameter is assumed to be small with respect to both the wavelength of the incident wave and the minimum distance between posts.

The impedance per unit length of a single post is first defined and calculated. Next, the sheet impedance of a single infinite row of identical posts is defined, and determined in terms of the impedance per unit length of the individual posts. The reflection from several rows of posts is then examined. An explicit formula for the reflection coefficient is obtained for the case where each row of the array is modelled as an impedance sheet. The limit where the impedance sheet concept breaks down is pointed out, and a method for extending the simpler results to this more general case is indicated.



Contents

I.	Introduction - - - - -	3
II.	Impedance Per Unit Length of a Single Dielectric Post- - - - -	9
III.	Sheet Impedance of an Infinite Row of Identical Posts- - - - -	20
IV.	Reflection From Several Uniformly Spaced Impedance Sheets- - - - -	30
V.	Reflection From Several Rows of Posts -- a More General Approach - - - -	57
VI.	Concluding Remarks - - - - -	63
	Appendix A - The Other Polarization- - - - -	66
	Appendix B - A Matrix Inversion- - - - -	77
	References - - - - -	81

Figures

1.	A possible design for ATLAS II - - - - -	4
2.	Cross-section of the idealized model for the trestle - - - - -	5
3.	Scattering from a single post- - - - -	10
4.	Magnitude of the relative error of (2.10) for circular posts - - - - -	17
5.	An infinite row of identical posts - - - - -	22
6.	Discreteness contribution to sheet impedance of a row of posts - - - - -	26
7.	Several uniformly spaced impedance sheets- - - - -	31
8.	$ R_{\infty} ^2$ (in percent) vs. $(2D/\lambda)$ for various values of α for an infinite number of sheets- - - - -	35
9.	Phase change per section of a wave in an infinite sheet medium - - - - -	42
10.	Decay constant per section in stop band of an infinite sheet medium- - -	43
11.	$100 R_N $ vs. $2D/\lambda$ for $N = 1$ and various α - - - - -	49
12.	$100 R_N $ vs. $2D/\lambda$ for $N = 2$ and various α - - - - -	50
13.	$100 R_N $ vs. $2D/\lambda$ for $N = 4$ and various α - - - - -	51
14.	$100 R_N $ vs. $2D/\lambda$ for $N = 8$ and various α - - - - -	52

Acknowledgement

Dr. C. E. Baum suggested looking into this problem. Mr. R. W. Sassman did the numerical work for Section V. Mrs. Georgene Peralta did the typing and drawing.

I. Introduction

It appears that the best way to determine the effect of the nuclear electromagnetic pulse on a large aircraft full of electronic equipment is to stick the large aircraft into a large simulator. The large simulators that have been proposed for this job have been designated ATLAS I and ATLAS II in previous notes in this series (see references [1] through [4] and also Section IV of reference [5]). These simulators are essentially parallel-plate transmission lines with appropriate source and termination regions. The electric field of ATLAS I will be horizontal; the electric field of ATLAS II will be vertical. The aircraft will be run out onto a platform supported between the two plates. Figure 1 is a sketch of a possible design for ATLAS II. This picture has been taken from reference [5].

A quick look at Figure 1 will reveal that, in addition to the aircraft, there is quite a bit of its support structure between the simulator plates. It would be nice if the aircraft would just float in the air between the plates, since that is the situation it is desirable to simulate. This being impossible, the next best thing will be done. The support structure will be a trestle, i.e., a sparse array of wooden beams. The average relative permittivity within the trestle will be close to unity. Thus the support structure will reflect very little energy in the low frequency limit. Nevertheless, there exists the possibility of enhanced reflections at higher frequencies, in particular at those frequencies where the length of the incident wave is the same as one of the characteristic lengths within the array of wood. At those frequencies, one might expect some sort of stop-band effect within the trestle, and thus a large amount of reflection of an incident wave. The purpose of this note is to examine this possibility and to present some basic data for estimating the importance of trestle reflection effects.

The effect of the trestle in Figure 1 can be estimated by studying the model shown in Figure 2. Figure 2 depicts several rows of infinitely long dielectric cylinders. The rows themselves are also infinitely long. The cross-sections of the cylinders may be of arbitrary shape, but all cross-sections are identical. A time-harmonic plane wave is incident normally on the first row of cylinders. The incident wave is plane polarized and its electric vector is parallel to the generators of the cylinders.

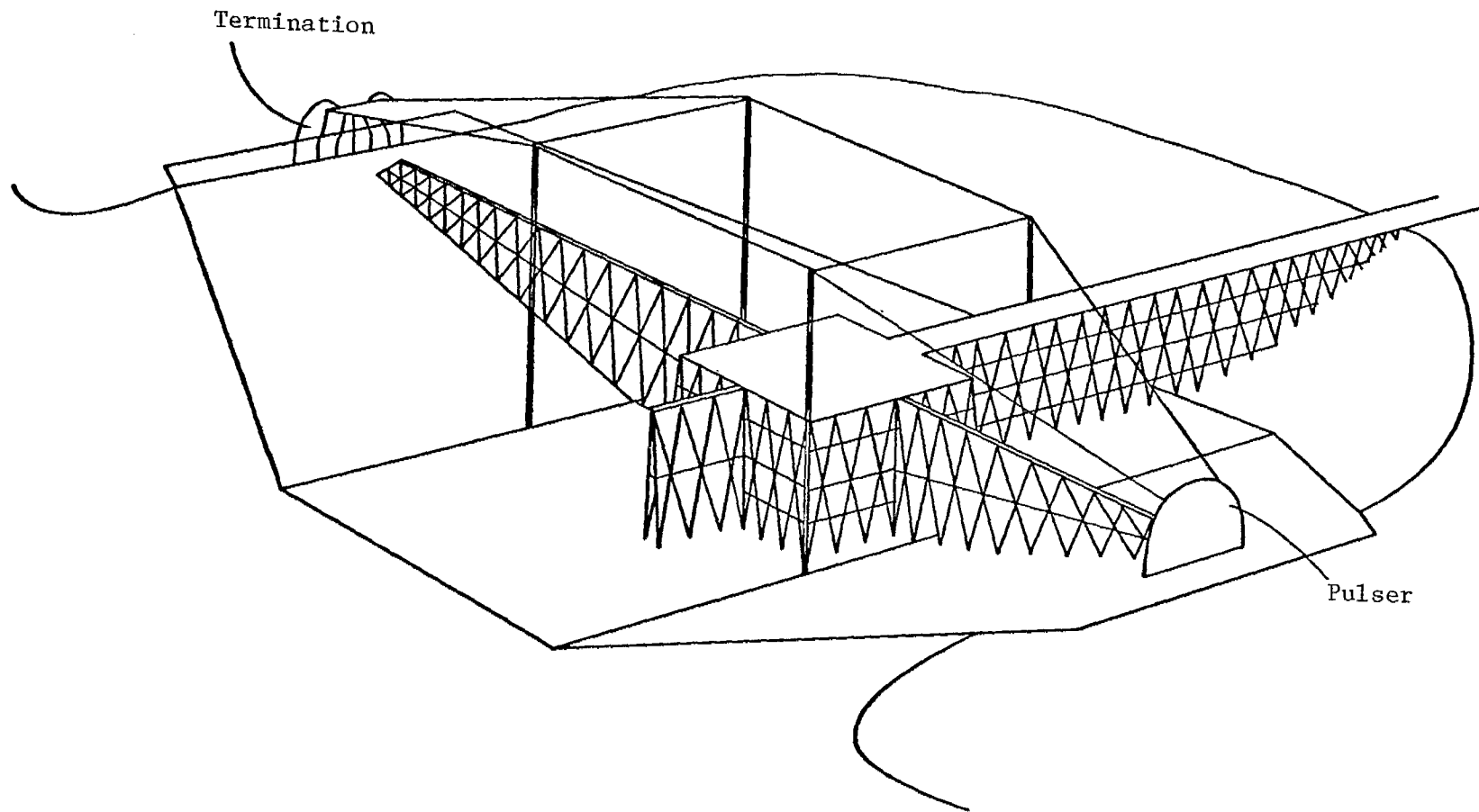


Figure 1. A possible design for ATLAS II.

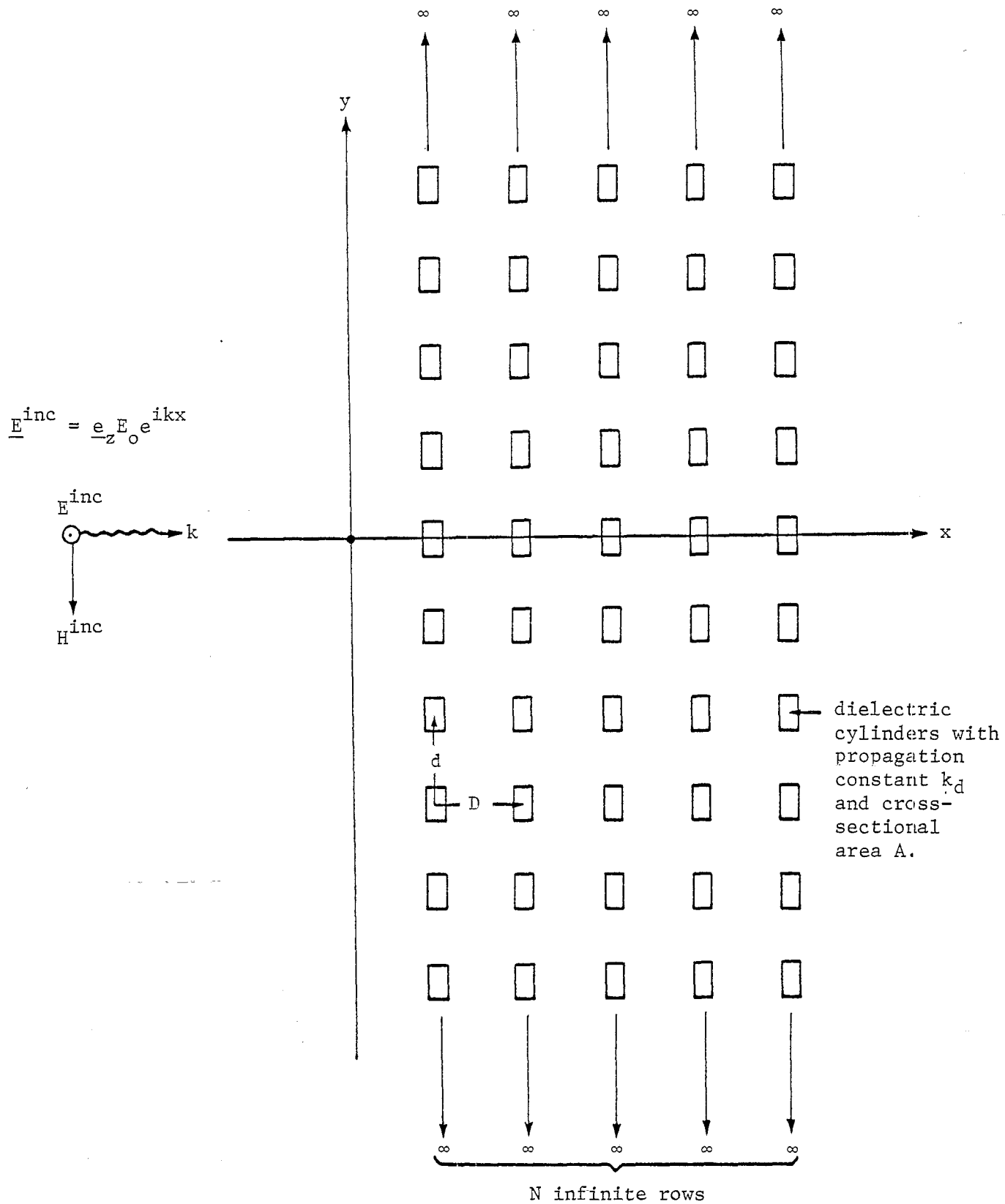


Figure 2. Cross-section of the idealized model for the trestle.

This model may be looked upon as a "worst case" model for two reasons. The first reason is that the reflected field just in front of an array of finite width and height (which would more accurately represent the real trestle) would seem clearly, on physical grounds, to be no greater than the reflected field of an array of infinite width and height. The second reason is that the wave reflected from an infinite array when the incident electric field is perpendicular to the generators of the dielectric cylinders will have a smaller amplitude than the wave reflected in the parallel polarization case to be studied in this note. Appendix A is a justification of this statement. Incidentally, Appendix A contains a proof of some interesting bounds on the diagonal elements of the polarizability tensor of a homogeneous dielectric body. Appendix A also contains a statement of two integral equations that can be used for the numerical computation of the elements of the polarizability tensor. One of these integral equations is not very well known.

For the two reasons mentioned in the preceding paragraph, the numerical values of the amplitude of the wave reflected from N infinite rows of infinite cylinders, which we will calculate in this note, can be looked upon as bounds on the magnitude of the actual reflected field just in front of a real trestle with N rows of posts.

In the rest of this note, the words "cylinder" and "post" will be used interchangeably in referring to the infinitely long dielectric cylinders of the idealized model.

There are two basic assumptions we will make in order to simplify the problem of calculating the wave reflected from the model array. These assumptions are quite compatible with the real situation that the model problem represents. The assumptions are:

- (1) The maximum diameter of any post is small compared to the wavelength of the incident wave.
- (2) The maximum diameter of any post is small compared to the minimum distance between posts.

The reasons for working under these assumptions will become clear as the work proceeds. In addition to these two basic assumptions, we will often make one,

or more, of three secondary assumptions in order to obtain simple explicit expressions for the quantities we wish to calculate. These secondary assumptions are:

- (3) If k is the free-space propagation constant corresponding to the frequency of the incident wave, k_d is the propagation constant within the dielectric of the posts, and A is the cross-sectional area of a post, then $(k_d^2 - k^2)A \ll 1$.
- (4) The distance between the rows of the array is not less than the distance between the individual posts in a row.
- (5) The distance between rows of posts and the distance between the individual posts in a single row are both less than the wavelength of the incident wave.

These three secondary assumptions are also compatible with the real situation in most cases of interest.

In this note we will talk a lot about the impedances of things -- of a single post, of a row of posts, etc. The reason for this is that a lot of people seem to have a certain amount of intuitive feeling for impedances, and this often makes equations involving them a little easier to absorb than the same equations written in terms of more fundamental physical parameters like length, permittivity, and frequency.

In the next section, we will define, and give a recipe for calculating, the impedance per unit length of a single post. We will give a simple approximate expression for this quantity which is accurate when assumption (3) is valid. Furthermore, we will calculate the precise error of the approximate expression when it is applied to the special case of a circular post.

In Section III, we will derive an expression for the equivalent sheet impedance of a single, uniformly spaced, row of posts in terms of the impedance per unit length of a single post in the row. This sheet impedance is defined as the sheet impedance of a uniform sheet having the same reflection and transmission coefficients as the actual row of posts. The connection of this sheet impedance with the well known sheet impedance of a wire grating will also be discussed.

In Section IV, we will calculate the reflection coefficient of N rows of posts when each row of posts is looked upon as a uniform sheet having a sheet impedance given by the expression derived in Section III. Under this assumption, we will be able to derive an explicit expression for the reflection coefficient. This explicit result depends on the exact inversion of a certain matrix. This inversion is performed in Appendix B. In Section IV, we will also derive an equation for the propagation constant of a wave traveling in an infinite medium made up of uniformly spaced impedance sheets. This propagation constant manifests the expected stop-band characteristics as peaks in its imaginary part.

In Section V, we will study the accuracy of the solution in Section IV by examining a more general formulation of the reflection coefficient problem, including the effects of non-TEM interactions between rows of posts. It turns out that this formulation gives rise to equations that reduce quite accurately to those solved in Section IV if assumption (4), concerning the relative distance between rows of posts and posts in a single row, is valid. Also, in this section we will give accurate numerical values of the propagation constant of a wave traveling in an infinite array of posts. In fact, the agreement between this propagation constant and the one calculated in Section IV will be used as a measure of the accuracy of the rest of the work of Section IV.

In the last section, we will extract whatever conclusions we can from the preceding analytical work. We will also point out some directions in which an extension of the analysis would seem to be fairly straightforward and useful.

II. Impedance Per Unit Length of a Single Dielectric Post

Let us consider the problem of calculating the wave scattered by a single dielectric post when an incident wave propagates in a direction perpendicular to the post and is polarized with its electric field parallel to the post. This essentially two-dimensional problem is shown schematically in Figure 3.

Conceptually, the easiest way to treat this problem is to note that the z component of the electric field satisfies the two-dimensional Helmholtz equation

$$\nabla^2 E_z(\underline{\rho}) + k_c^2 E_z(\underline{\rho}) = 0 \quad (2.1)$$

where

$$k_c^2 = k^2 = \omega^2 \mu_0 \epsilon_0 \quad \text{outside the post}$$

$$k_c^2 = k_d^2 = \omega^2 \mu_0 \epsilon(\underline{\rho}) \quad \text{within the post}$$

and $\underline{\rho}$ is the two-dimensional position vector.

We can rewrite equation (2.1) as

$$\nabla^2 E_z(\underline{\rho}) + k^2 E_z(\underline{\rho}) = -(k_c^2 - k^2) E_z(\underline{\rho}) \quad (2.2)$$

where the right hand side is nonzero only within the post. If we consider the right hand side of equation (2.2) as known, we can call upon the two-dimensional Green's function for the Helmholtz equation (reference [6], p. 811) and write

$$E_z(\underline{\rho}) = E_z^{\text{inc}}(\underline{\rho}) + \frac{i}{4} \int_A (k_c^2 - k^2) H_0^{(1)}(k|\underline{\rho} - \underline{\rho}'|) E_z(\underline{\rho}') dS' \quad (2.3)$$

This equation is really an integral equation for the determination of $E_z(\underline{\rho})$ within the post. Its numerical solution has been discussed by Richmond [7].

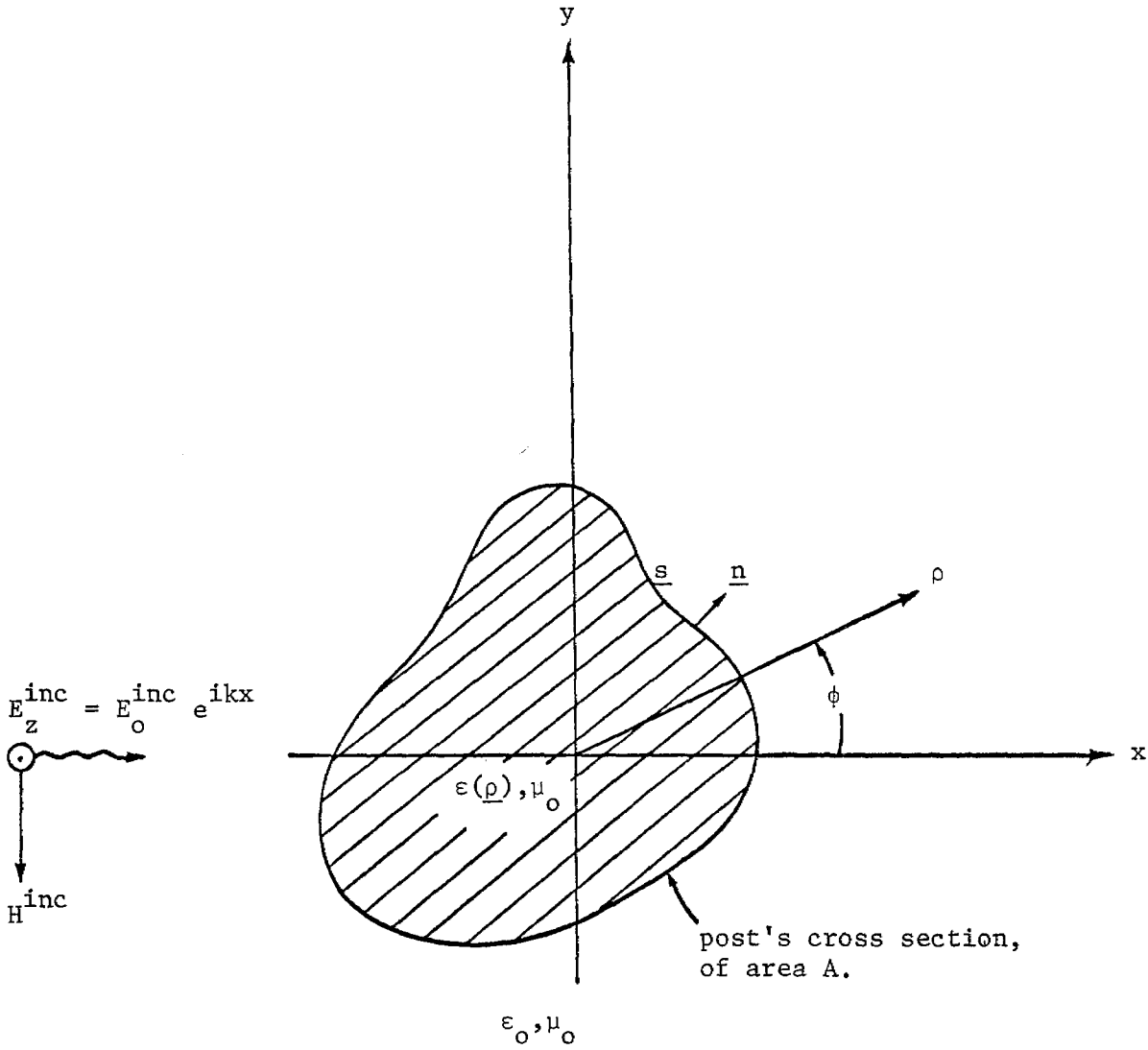


Figure 3. Scattering from a single post.

The integral in equation (2.3) is the scattered field. If $|\underline{\rho}|$ is greater than the maximum $|\underline{\rho}'|$ within the post, this scattered field may be rewritten as

$$E_z^S(\underline{\rho}) = \frac{ik^2}{4} \sum_{m=-\infty}^{\infty} H_m^{(1)}(k\rho) e^{im\phi} \int_A J_m(k\rho') e^{-im\phi'} [\epsilon_r(\underline{\rho}') - 1] E_z(\underline{\rho}') dS' \quad (2.4)$$

where

$$\epsilon_r(\underline{\rho}) = \epsilon(\underline{\rho})/\epsilon_0.$$

We now recall our first basic assumption, which implies that, within the range of integration of equation (2.4),

$$k\rho' \ll 1$$

as long as the origin of the two-dimensional coordinate system is chosen somewhere near the center of gravity of the cross section of the post. From the small argument asymptotic forms of the Bessel functions, it is then clear that it is only necessary to keep the $m = 0$ term in the sum, and thus

$$E_z^S(\underline{\rho}) \approx \frac{ik^2}{4} H_0^{(1)}(k\rho) \int_A [\epsilon_r(\underline{\rho}') - 1] E_z(\underline{\rho}') J_0(k\rho') dS'. \quad (2.5)$$

But the electric field due to a line current, I , flowing along the z -axis is given by

$$E_z(\rho) = -\frac{\omega\mu_0 I}{4} H_0^{(1)}(k\rho), \quad (2.6)$$

thus the scattered field given by equation (2.5) can be thought of as being due to an equivalent line current of strength

$$I_{eq} = -i\omega \int_A [\epsilon(\underline{\rho}') - \epsilon_0] E_z(\underline{\rho}') J_0(k\rho') dS'.$$

Now, according to our first basic assumption, the incident field will not vary much over the post's cross section, and so

$$E_z^{\text{inc}}(\underline{\rho}) \approx E_z^{\text{inc}}(0) \equiv E_0^{\text{inc}} \quad (2.7)$$

On the other hand, if $\epsilon_r(\underline{\rho})$ is large, $E_z(\underline{\rho}')$ could vary quite a bit over the range of integration, but it will be linearly proportional to E_0^{inc} . Thus the ratio

$$\frac{I_{\text{eq}}}{E_0^{\text{inc}}} = -i\omega\epsilon_0 \int_A [\epsilon_r(\underline{\rho}) - 1][E_z(\underline{\rho}')/E_0^{\text{inc}}] J_0(k\rho') dS' \quad (2.8)$$

will be independent of the amplitude of the incident field (and, according to equation (2.7), also independent of its precise spatial variation). The reciprocal of equation (2.8) has the dimensions of impedance per unit length; this impedance is the impedance to the flow of the current generating the scattered field. We will denote this impedance by Z_p and its reciprocal (i.e., the ratio given by equation (2.8) itself) as Y_p .

In the rest of this note, we will make a great deal of use of a special case of equation (2.8). This special case is the one where assumption (3) of Section I is valid, i.e.,

$$(k_d^2 - k^2)A \ll 1.$$

Under this assumption, it easily follows from equation (2.3) that

$$E_z(\underline{\rho}) \approx E_z^{\text{inc}}(\underline{\rho}) = E_0^{\text{inc}}$$

within the post, and thus (since $J_0(k\rho) \approx 1$)

$$Z_p^{-1} = Y_p = -i\omega\epsilon_0 \int_A [\epsilon_r(\underline{\rho}) - 1] dS'. \quad (2.9)$$

If, furthermore, the post can be considered to be homogeneous (this will be the case for the real wooden beams we are concerned with), the above formula simplifies to

$$Z_p^{-1} = Y_p = -i\omega A(\epsilon - \epsilon_0), \quad (2.10)$$

and, according to equation (2.6), the scattered field is given by

$$\begin{aligned} E_z^S(\rho) &= -\frac{\omega\mu_0}{4} Y_p E_0^{inc} H_0^{(1)}(k\rho) \\ &= \frac{ik^2 A}{4} (\epsilon_r - 1) E_0^{inc} H_0^{(1)}(k\rho) \end{aligned} \quad (2.11)$$

Before proceeding further, let us interpret equation (2.10) physically. It's not hard. Equation (2.10) is just the difference between the capacitive admittance between two cross sections of the post a unit distance apart and the capacitive admittance between the same cross sections with the dielectric post absent ("fringing" fields are not present in the problem we are considering). It is the current through this extra admittance that gives rise to scattered fields.

Equation (2.11) holds as long as ρ is much greater than the maximum diameter of the post's cross section (ρ does not have to be large compared to λ). This equation corresponds to a scattering width given by

$$\sigma^{sc} = \lim_{\rho \rightarrow \infty} \frac{\int E_z^S(\rho, \phi) E_z^{S*}(\rho, \phi) \rho d\phi}{|E_z^{inc}|^2} = (\epsilon_r - 1)^2 \frac{k^3 A^2}{4}$$

This result has been derived by Van Bladel [8], [9].

For the case where the cylinder is circular, equation (2.11) gives

$$\frac{E_z^S(\rho)}{E_0^{inc}} = \frac{i\pi}{4} (ka)^2 (\epsilon_r - 1) H_0^{(1)}(k\rho)$$

This approximation to the field scattered from a homogeneous circular cylinder

has been called the "dielectric needle" limit by Van de Hulst [10]. Its accuracy has been discussed by Kerker, et al [11], who have drawn equal error contours in the $ka - \sqrt{\epsilon_r}$ plane for $k\rho$ large and various values of ϕ . We prefer here to make use of the analytic solution to the circular cylinder problem to exhibit the error in the simple expression (2.10) as an approximation to the exact expression (2.8). Hopefully, the error in expression (2.10) for other cross-sectional shapes will be in the same ball park as the one we calculate if we use something like $k(A/\pi)^{1/2}$ as the appropriate value for ka .

From equation (2.8) and the analytical solution of the circular cylinder problem (see, for example, reference [12], §8.6), we can write

$$Y_p = -i\omega(\epsilon - \epsilon_o)2\pi C_o \int_0^a J_o(k\rho)J_o(k_d\rho)\rho d\rho$$

where

$$C_o = (2i/\pi)[k_d a J_1(k_d a)H_o^{(1)}(ka) - ka J_o(k_d a)H_1^{(1)}(ka)]^{-1}.$$

carrying out the integration (the integral is a special case of one given in reference [13], p. 484), and simplifying, Y_p can be written as

$$Y_p = -i\omega(\epsilon - \epsilon_o)A \frac{4i}{\pi x^2 (\eta^2 - 1)} \left\{ \frac{\eta J_o(x)J_1(\eta x) - J_o(\eta x)J_1(x)}{\eta J_1(\eta x)H_o^{(1)}(x) - J_o(\eta x)H_1^{(1)}(x)} \right\} \quad (2.12)$$

where

$$x \equiv ka$$

and

$$\eta \equiv (\epsilon_r)^{1/2}$$

From (2.10) and (2.12), it is easy to arrive at the following expression for $R(x, \eta)$, the relative error of formula (2.10)

$$R(x, \eta) = \left\{ \frac{\pi x^2 (\eta^2 - 1)}{4} \left[\frac{J_0(\eta x) Y_1(x) - Y_0(x) J_1(\eta x)}{J_0(\eta x) J_1(x) - J_0(x) J_1(\eta x)} \right] - 1 \right\} - \frac{i \pi x^2 (\eta^2 - 1)}{4} \quad (2.13)$$

The magnitude of this relative error is given, as a percentage, in Table 1 and Figure 4. From this data we can see that for the wooden posts we are interested in (ϵ_r about 4 or 5) there will not be much error in equation (2.10) as long as ka is less than .1. For the rest of this note, whenever it comes to calculating specific numbers, we will therefore use the approximate expression (2.10).

Nevertheless, for the sake of completeness, we will give a brief outline of how one could calculate Z_p (or Y_p) if assumption (3) (equivalent to equation (2.10) for homogeneous posts), were invalid. There are, in fact, several alternatives. If the post is inhomogeneous, the best way would probably be to solve equation (2.3) in some manner such as that used by Richmond [7], and then to use the solution to evaluate equation (2.8) numerically. (Note that under the first basic assumption it is not really necessary to keep the Bessel function in the integrand of equation (2.8); we can set it equal to 1).

If the post is homogeneous, the above method is not necessary and it would be quite wasteful of computer time. What one really should do for homogeneous posts is to look for an appropriate line integral equation over the boundary of the post's cross section, or some other numerical method that makes maximum use of the homogeneity of the post (one such other method, due to D. R. Wilton [14], is quite new). If one prefers the line integral equation method, he must be satisfied with a pair of coupled equations for $E_z(s)$ and $(\partial/\partial n)E_z(s)$, where \underline{n} is the outward normal shown in Figure 3. Based on a two-dimensional Maue representation for $(\partial/\partial n)E_z(s)$ [15], one way of writing this pair of coupled equations would be

$$E_z(s) = E_z^{inc}(s) - \int_C [G^i(\underline{\rho}, \underline{\rho}') - G^o(\underline{\rho}, \underline{\rho}')]_{\underline{n}} E_z(s') - [G^i(\underline{\rho}, \underline{\rho}') - G^o(\underline{\rho}, \underline{\rho}')]_{E_{zn}'}(s') ds' \quad (2.14)$$

and

Table 1. Magnitude of the relative error of equation (2.10)
for the case of circular posts (in percent).

ϵ_r x	1	2	3	4	5	6	7	8	9	10
.01		.02	.05	.08	.10	.13	.15	.18	.21	.23
.02	.01	.08	.17	.26	.36	.45	.54	.63	.72	.81
.03	.02	.17	.36	.54	.73	.92	1.11	1.30	1.48	1.67
.04	.04	.28	.59	.90	1.22	1.53	1.84	2.16	2.47	2.78
.05	.06	.41	.87	1.34	1.80	2.26	2.73	3.19	3.65	4.12
.06	.09	.56	1.20	1.84	2.47	3.11	3.75	4.39	5.03	5.67
.07	.12	.73	1.56	2.40	3.23	4.07	4.90	5.74	6.57	7.41
.08	.16	.92	1.99	3.02	4.07	5.13	6.18	7.23	8.28	9.34
.09	.20	1.12	2.41	3.70	4.99	6.28	7.57	8.86	10.15	11.44
.10	.25	1.34	2.88	4.44	5.98	7.53	9.08	10.62	12.17	13.72

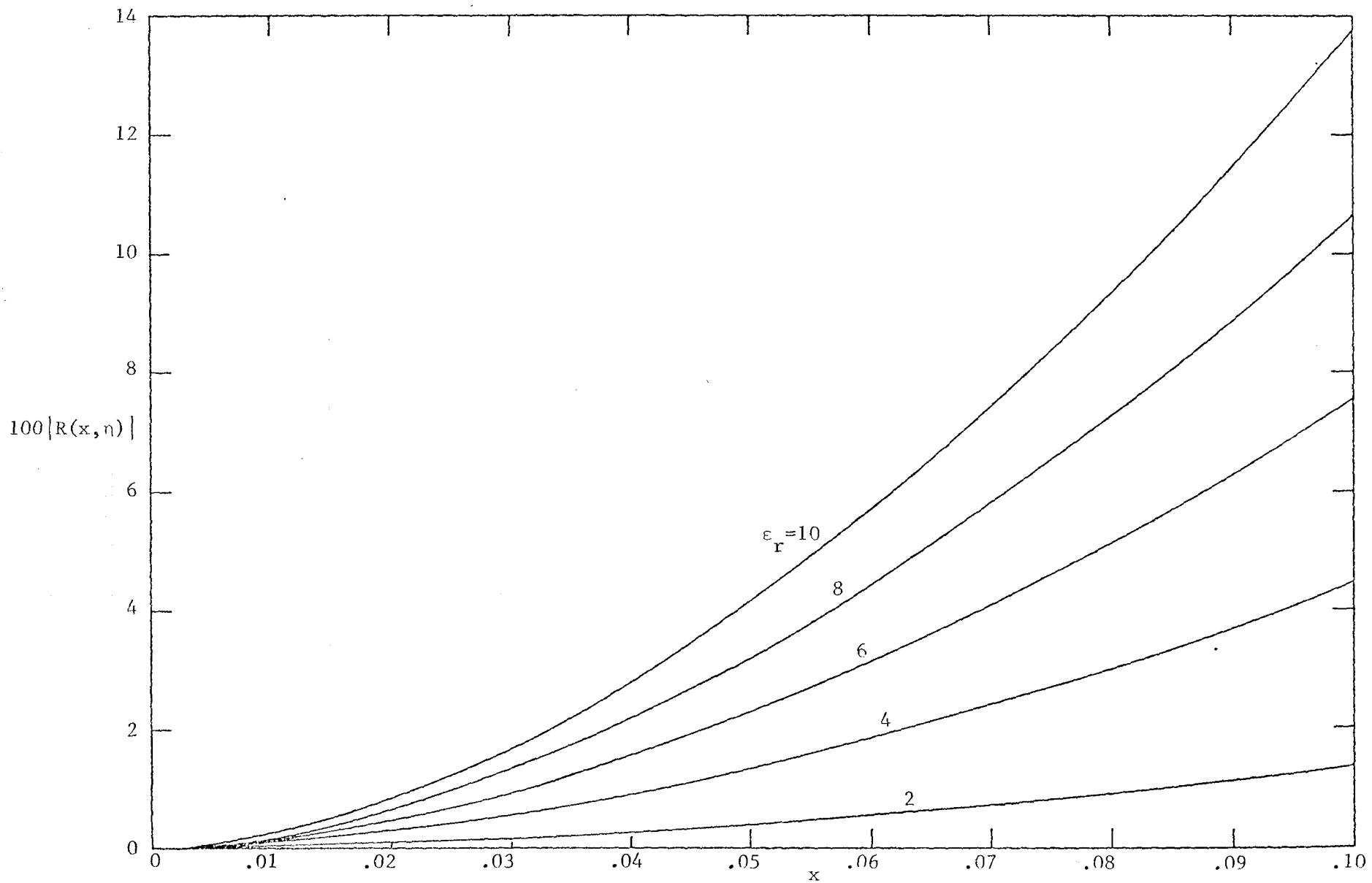


Figure 4. Magnitude of the relative error of (2.10) for circular posts.

$$\begin{aligned}
E_{zn}(s) = E_{zn}^{inc}(s) - \int_c \left\{ [G^i(\underline{\rho}, \underline{\rho}') - G^o(\underline{\rho}, \underline{\rho}')] \right. \\
- [G^i(\underline{\rho}, \underline{\rho}') - G^o(\underline{\rho}, \underline{\rho}')]_n E_{zn'}(s') \left. \right\} ds' \\
- \int_c [k_d^2 G^i(\underline{\rho}, \underline{\rho}') - k^2 G^o(\underline{\rho}, \underline{\rho}')] (\underline{n} \cdot \underline{n}') E_z(s') ds' \quad (2.15)
\end{aligned}$$

where

$$G^o(\underline{\rho}, \underline{\rho}') = \frac{i}{4} H_0^{(1)}(k|\underline{\rho} - \underline{\rho}'|)$$

$$G^i(\underline{\rho}, \underline{\rho}') = \frac{i}{4} H_0^{(1)}(k_d|\underline{\rho} - \underline{\rho}'|)$$

and where the subscripts n and s denote partial derivatives in the normal and tangential directions (see Figure 3). When equations (2.14) and (2.15) have been solved numerically, the surface integral representation for Y_p , equivalent to equation (2.8),

$$Y_p = - \frac{i\omega\epsilon_0}{E_o^{inc}} \int_c \left\{ E_z(s) [J_o(k\rho)]_n - J_o(k\rho) E_{zn}(s) \right\} ds \quad (2.16)$$

may be used. For small posts (i.e., under assumption (1)), equation (2.16) reduces to

$$Y_p = - \frac{i\omega\epsilon_0 k^2}{E_o^{inc}} \left\{ - \int_c (\rho^2)_n E_z(s) ds - \frac{1}{k^2} \int_c E_{zn}(s) ds \right\}. \quad (2.17)$$

If, furthermore, ϵ_r is not too large, we may replace $E_z(s)$ by E_o^{inc} in the first integral of equation (2.17) (reducing that integral to $A E_o^{inc}$), and replace the second integral by

$$\begin{aligned}
\int_C \mathbf{E}_{zn}(s) ds &= \int_C \mathbf{n} \cdot \nabla \mathbf{E}_z(\rho) ds \\
&= \int_A \nabla^2 \mathbf{E}_z(\rho) dS \\
&= -k_d^2 \int_A \mathbf{E}_z(\rho) dS \\
&\approx -k_d^2 \mathbf{A} \mathbf{E}_o^{\text{inc}}
\end{aligned}$$

These substitutions thus reduce equation (2.17) back to equation (2.10).

In concluding this discussion of line integral equations, it might be well to point out that equations (2.14) and (2.15) are equivalent to the two-dimensional form of Müller's integral equations [16], [17], and that there are an infinite number of other equivalent pairs of equations, (see the elegant discussion by Mitzner [18]).

III. Sheet Impedance of an Infinite Row of Identical Posts

Let us now turn to the calculation of the equivalent sheet impedance of a single row of identical posts. In order to do this we must first state exactly what we mean by "sheet impedance" and what we mean by "equivalent."

The sheet impedance of an infinitesimally thin impedance sheet is equal to the ratio of the tangential electric field at the surface of the sheet to the jump in magnetic field through the sheet. This definition assumes the continuity of the tangential electric field through the sheet and implies a sheet current flowing in the sheet. The sheet impedance concept has useful applications in modelling the electromagnetic properties of several real objects such as low-frequency shields [19] and the terminations of transmission-line simulators [20], [21].

The equivalent sheet impedance of our row of posts is the sheet impedance of the uniform impedance sheet that will give rise to the same electric field reflection coefficient for a normally incident plane wave as our "discrete sheet" of dielectric posts gives rise to. This equality of reflection coefficients is used in our definition of "equivalent" because it leads, when we model several rows of posts by several sheets in Section IV, to the exact results if the row spacing is much larger than the interpost spacing.

For comparison purposes, therefore, we must first know the reflection coefficient of a uniform impedance sheet having sheet admittance Y_s . We assume the impedance sheet to be in the y - z plane and the incident electric field to be of the form

$$\underline{E}^{\text{inc}} = \underline{e}_z E_0^{\text{inc}} e^{ikx}.$$

By the definition of Y_s and R , the sheet current, \underline{K} , is given by

$$\underline{K}_z = (1 + R) E_0^{\text{inc}} Y_s \quad (3.1)$$

while the electric field generated by this current is easily shown to be

$$E_z^s = -\frac{K Z_0}{2} e^{ik|x|} \quad (3.2)$$

where $Z_0 = (\mu_0/\epsilon_0)^{1/2}$ is the impedance of free space. Now for negative x we have

$$E_z^s = E_z^{\text{ref}} = -\frac{K Z_0}{2} e^{-ikx} = R E_0^{\text{inc}} e^{-ikx}. \quad (3.3)$$

Therefore, substituting equation (3.1) into equation (3.3) we get

$$-\frac{(1+R)Y_s Z_0}{2} = R$$

Thus, if $y_s \equiv Y_s/Y_0 \equiv Y_s Z_0$, we can see that

$$y_s = -\frac{2R}{1+R}$$

or

$$R = -\frac{y_s}{2+y_s} \quad (3.4)$$

Now let us calculate the actual reflection coefficient of the row of posts in Figure 5, and equate it to the R of equation (3.4) in order to determine the row's equivalent sheet impedance. In order to do this we will invoke the two basic assumptions of Section I.

The equivalent current in the post at position $(0,md)$ will be

$$I_{\text{eq}} = Y_p E_z(0,md), \quad (3.5)$$

while the field scattered by the post at position $(0,md)$ will be, from equation (2.6),

$$E_m^s(x,y) = -\frac{\omega \mu_0 I_{\text{eq}}}{4} H_0^{(1)}(\sqrt{k^2 x^2 + (y - md)^2}) \quad (3.6)$$

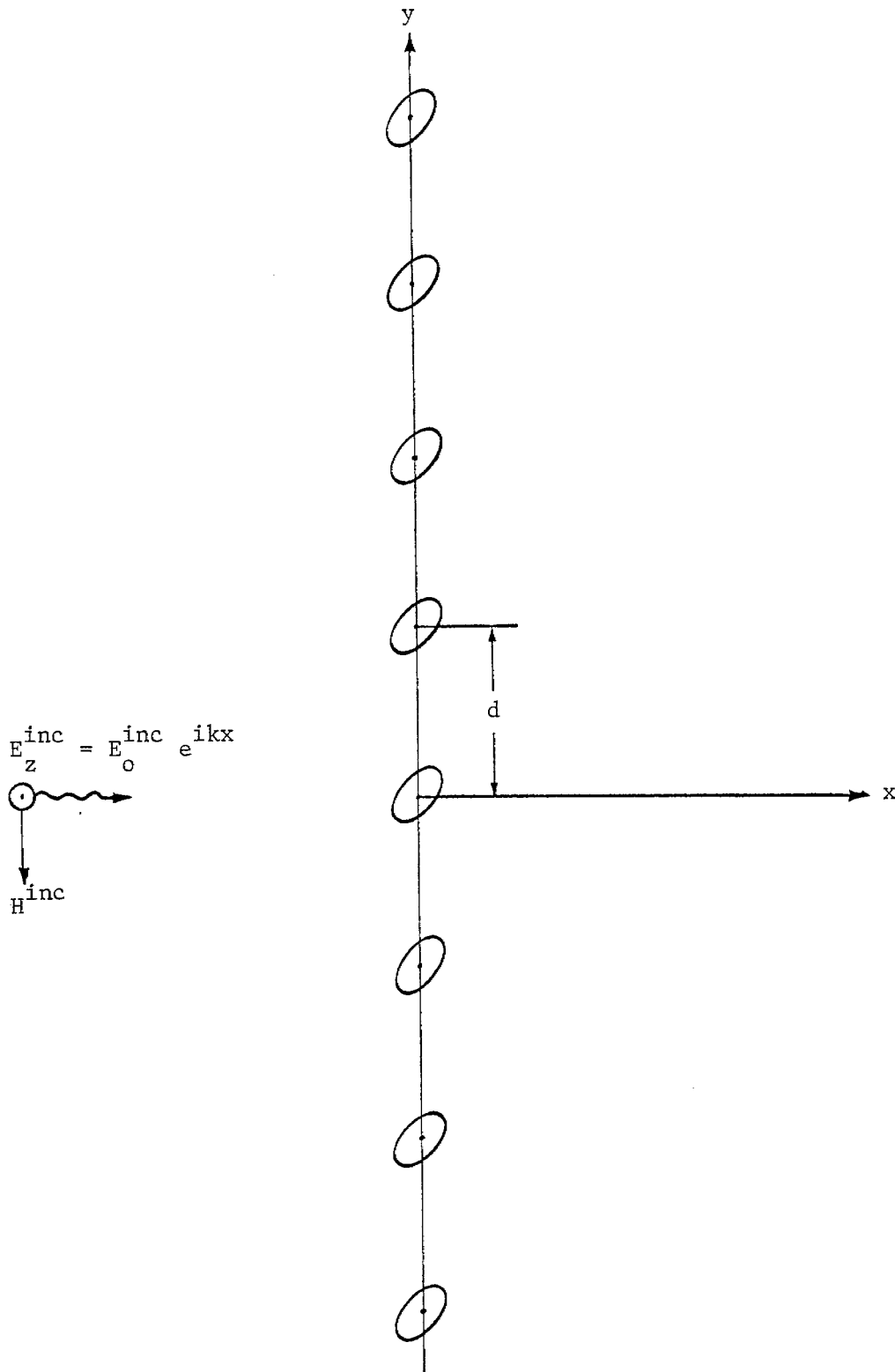


Figure 5. An infinite row of identical posts.

But

$$E_z(0,nd) = E^{\text{inc}}(0,nd) + \sum_{m=-\infty}^{\infty} E_m^s(0,nd) \quad (3.7)$$

where the prime on the summation means that the $n = m$ term is omitted. From equations (3.6) and (3.7) we can write

$$E_z(0,nd) = E^{\text{inc}}(0,nd) - \frac{\omega\mu_o I_{\text{eq}}}{2} \sum_{m=1}^{\infty} H_o^{(1)}(mkd) \quad (3.8)$$

or, defining

$$S_1 = \sum_{m=1}^{\infty} H_o^{(1)}(mkd), \quad (3.9)$$

and using equation (3.5), we have

$$I_{\text{eq}} = Y_p \left\{ E_o^{\text{inc}} - \frac{\omega\mu_o I_{\text{eq}}}{2} S_1 \right\}. \quad (3.10)$$

If we define an equivalent sheet current, K_{eq} , through

$$K_{\text{eq}} \equiv I_{\text{eq}}/d, \quad (3.11)$$

equation (3.10) can be rewritten as

$$K_{\text{eq}} = (Y_p/d) \left\{ E_o^{\text{inc}} - \frac{kdK_{\text{eq}}Z_o}{2} S_1 \right\}, \quad (3.12)$$

i.e.,

$$K_{\text{eq}} = \frac{(Y_p/d)E_o^{\text{inc}}}{1+(Y_p/d)Z_o(kdS_1/2)}. \quad (3.13)$$

Identifying the sheet current of equation (3.3) with the K_{eq} of equation (3.13), we can already write

$$R = - \frac{(Y_p Z_o / d)}{2 + Y_p Z_o (kdS_1) / d} \quad (3.14)$$

A justification of the identification of K_{eq} with the K of equation (3.3) can be arrived at by noting that, from equations (3.6) and (3.7), the reflected field is

$$E^{ref} = - \frac{\omega \mu_o I_{eq}}{4} \sum_{\text{all } m} H_o^{(1)}(k\sqrt{x^2 + (y - md)^2}). \quad (3.15)$$

This series may be transformed by using the Poisson summation formula to obtain [22]

$$E^{ref} = - \frac{Z_o I_{eq} e^{ik|x|}}{2d} + \frac{\omega \mu_o I_{eq}}{2} \sum_{m=1}^{\infty} \frac{e^{2\pi imY/d} e^{-2\pi\sqrt{m^2 - (kd/2\pi)^2}|x|/d}}{\sqrt{m^2 - (kd/2\pi)^2}} \quad (3.16)$$

The entire sum in equation (3.16) is rapidly decaying as $|x|$ increases (in fact, when we approximate several rows of posts by several uniform sheets in Section IV, what the approximation really amounts to is neglecting the contribution of this sum of evanescent modes to the fields at other rows of posts) and so we can identify the reflected field with the first term on the right hand side of equation (3.16). Thus

$$RE_o^{inc} = - \frac{Z_o I_{eq}}{2d} = - \frac{K_{eq} Z_o}{2}, \quad (3.17)$$

and this justifies our previous identification of K_{eq} with the K of equation (3.3) in arriving at equation (3.14).

Now, to get the equivalent sheet impedance of our row of posts, let us identify the reflection coefficients of equations (3.4) and (3.14). This identification is in accordance with our definition of equivalent sheet impedance. Let us also use the notation

$$y_p \equiv (Y_p Z_o / d).$$

Thus we have

$$\frac{y_s}{2+y_s} = \frac{y_p}{2+y_p(kdS_1)} \quad (3.18)$$

and this gives

$$y_s = \frac{2y_p}{2+y_p(kdS_1-1)} \quad (3.19)$$

or, denoting y_p^{-1} by z_p and y_s^{-1} by z_s ,

$$z_s = z_p + \frac{kdS_1-1}{2} \quad (3.20)$$

In equation (3.20), z_p is the sheet impedance of that uniform sheet that would be the result of spreading the dielectric material of the posts into a uniform sheet. (This identification presupposes the applicability of secondary assumption (3) of the introduction). Thus the second term on the right hand side of equation (3.20) is the "discreteness contribution" to the equivalent sheet impedance of a row of posts. This term is a function of kd only. Sums such as S_1 (and that of equation (3.15)) have been discussed frequently in the literature on scattering by gratings and grids (references [22] through [39] are a sampling of this literature; in grating applications, the discreteness contribution to z_s is relatively more important than in our dielectric post case, because the z_p of wire gratings can be quite small). By referring to reference [23] we can rewrite the discreteness contribution to z_s in the form

$$F(kd) \equiv \frac{kdS_1-1}{2} = -\frac{kd}{4} - \frac{ikd}{2\pi} \left\{ \gamma + \ln\left(\frac{kd}{4\pi}\right) + \sum_{n=1}^{\infty} \left[\frac{1}{\sqrt{n^2 - (kd/2\pi)^2}} - \frac{1}{n} \right] \right\} \quad (3.21)$$

which is valid for $kd < 2\pi$ (i.e., $d < \lambda$, secondary assumption (5) of Section I).

Table 2 is a table of $\text{Im } F(kd)$ vs. d/λ and vs. kd . A plot of $\text{Im } F(kd)$ vs. d/λ is given as figure 6. From this data, and equation (2.10) rewritten in the form

$$z_p = \frac{id}{\omega A(\epsilon - \epsilon_0) Z_0} = \frac{i}{kd(\eta^2 - 1)} \left(\frac{d}{A}\right)^2, \quad (3.22)$$

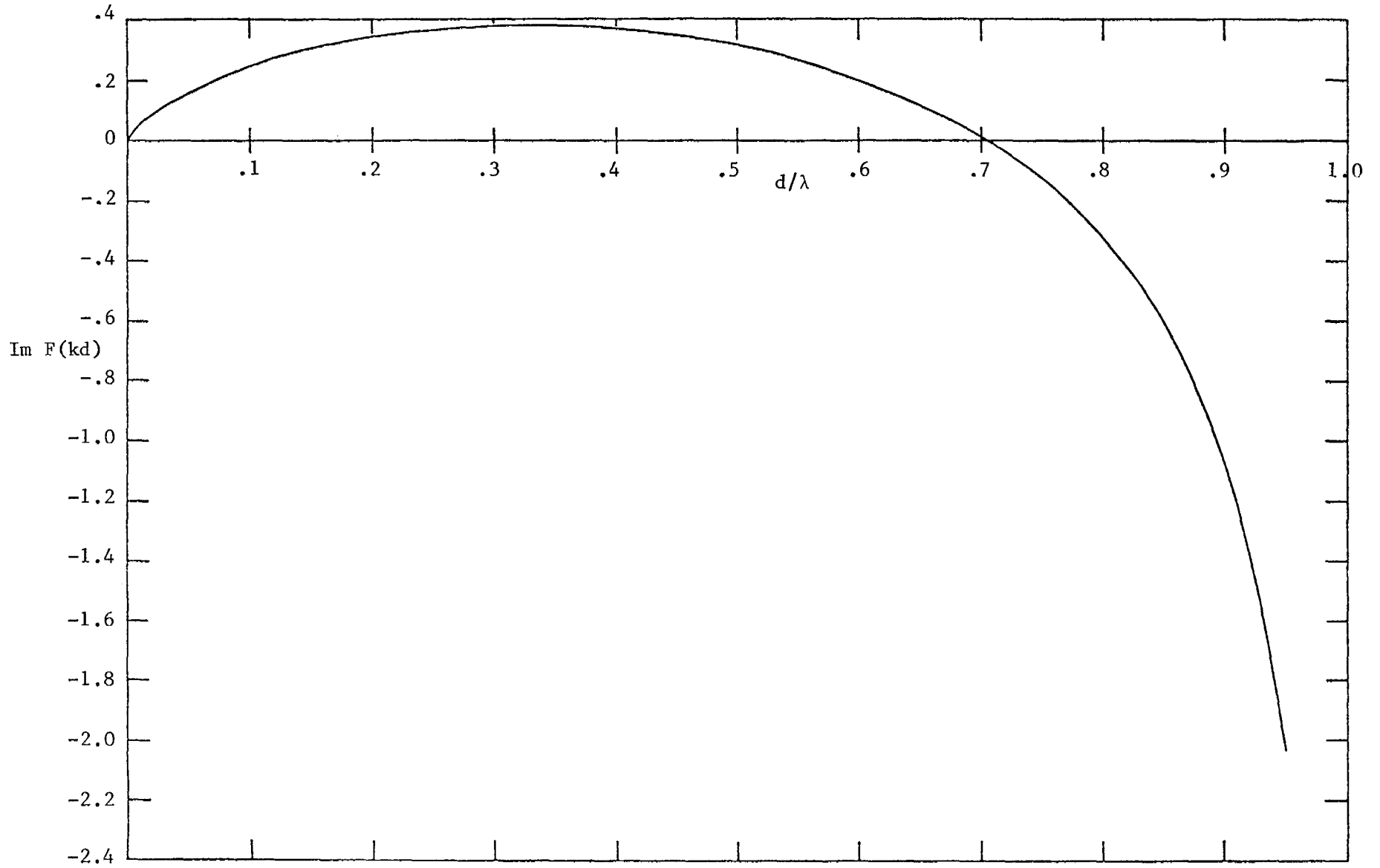


Figure 6. Discreteness contribution to sheet impedance of a row of posts.

Table 2a. Im F(kd) vs. d/λ

d/λ	Im F(kd)	d/λ	Im F(kd)	d/λ	Im F(kd)	d/λ	Im F(kd)
.01	.04721	.26	.36933	.51	.30572	.76	-.16098
.02	.08055	.27	.37240	.52	.29679	.77	-.19665
.03	.10866	.28	.37498	.53	.28727	.78	-.23469
.04	.13335	.29	.37709	.54	.27718	.79	-.27536
.05	.15551	.30	.37872	.55	.26647	.80	-.31897
.06	.17563	.31	.37989	.56	.25514	.81	-.36586
.07	.19406	.32	.38060	.57	.24316	.82	-.41646
.08	.21102	.33	.38085	.58	.23051	.83	-.47126
.09	.22671	.34	.38064	.59	.21716	.84	-.53088
.10	.24125	.35	.37998	.60	.20308	.85	-.59606
.11	.25475	.36	.37886	.61	.18824	.86	-.66775
.12	.26730	.37	.37729	.62	.17260	.87	-.74710
.13	.27896	.38	.37526	.63	.15614	.88	-.83565
.14	.28982	.39	.37278	.64	.13880	.89	-.93537
.15	.29990	.40	.36984	.65	.12054	.90	-1.04891
.16	.30926	.41	.36644	.66	.10130	.91	-1.17993
.17	.31793	.42	.36257	.67	.08104	.92	-1.33363
.18	.32595	.43	.35823	.68	.05968	.93	-1.51772
.19	.33334	.44	.35342	.69	.03717	.94	-1.74421
.20	.34014	.45	.34812	.70	.01341	.95	-2.03316
.21	.34635	.46	.34234	.71	-.01168	.96	-2.42120
.22	.35200	.47	.33605	.72	-.03819	.97	-2.98478
.23	.35712	.48	.32926	.73	-.06624	.98	-3.92173
.24	.36170	.49	.32195	.74	-.09596	.99	-6.01747
.25	.36577	.50	.31411	.75	-.12749	1.00	-∞

Table 2b. Im F(kd) vs. kd

kd	Im F(kd)	kd	Im F(kd)
.1	.06774	3.2	.30633
.2	.11340	3.3	.29190
.3	.15071	3.4	.27600
.4	.18256	3.5	.25856
.5	.21033	3.6	.23949
.6	.23483	3.7	.21870
.7	.25657	3.8	.19607
.8	.27592	3.9	.17147
.9	.29316	4.0	.14476
1.0	.30849	4.1	.11575
1.1	.32208	4.2	.08425
1.2	.33404	4.3	.05000
1.3	.34449	4.4	.01272
1.4	.35350	4.5	-.02793
1.5	.36115	4.6	-.07238
1.6	.36748	4.7	-.12112
1.7	.37256	4.8	-.17478
1.8	.37640	4.9	-.23413
1.9	.37905	5.0	-.30017
2.0	.38051	5.1	-.37414
2.1	.38081	5.2	-.45773
2.2	.37996	5.3	-.55315
2.3	.37796	5.4	-.66352
2.4	.37481	5.5	-.79324
2.5	.37050	5.6	-.94894
2.6	.36502	5.7	-1.14099
2.7	.35836	5.8	-1.38697
2.8	.35049	5.9	-1.71952
2.9	.34139	6.0	-2.20871
3.0	.33103	6.1	-3.04505
3.1	.31936	6.2	-5.08294

it is apparent that at low frequencies $F(kd)$ is negligible compared to z_p and that, if $(n^2 - 1)A/d^2$ is small, the region where $F(kd)$ is negligible could well include the entire region $kd < 2\pi$. In conjunction with the results in Appendix A on the relative reflection coefficients of the two polarizations of the incident field, this leads us to state that an approximate upper bound on the reflection coefficient of a trestle array can be obtained by assuming all the dielectric material to be concentrated in uniform sheets, spaced with a periodicity equal to the actual trestle periodicity in the direction of propagation of the incident wave.

IV. Reflection From Several Uniformly Spaced Impedance Sheets

This section consists of a calculation of the reflection coefficient of several uniformly spaced impedance sheets. There are alternative approaches to this calculation. We will follow the ones that seem, to us, to follow the actual physics of the problem most closely.

The problem to be solved is shown schematically in figure 7, which indicates the coordinate system and notation to be used.

First, we will solve the problem where N is infinite, i.e., we will determine the reflection from an infinite half-space of impedance sheets. The answer to this problem can be written down immediately, by using physical arguments, once we define the reflection and transmission coefficients of a single sheet as r and t and the intersheet phase factor, e^{ikD} , as p . The total reflection coefficient of the half-space is then

$$R_{\infty} = r + tpR_{\infty}pt + tpR_{\infty}prpR_{\infty}pt + tpR_{\infty}prpR_{\infty}prpR_{\infty}pt + \dots \quad (4.1)$$

where the first term, r , is due to the reflection from the first sheet. The next term, $tpR_{\infty}pt$, takes care of the wave that is transmitted through the first sheet, is reflected at the second sheet (note that R_{∞} is the same at the second sheet as at the first sheet -- it still is the front sheet of an infinite number of sheets), and then is transmitted back through the first sheet. Subsequent terms account for the infinite number of multiple reflections that can occur between the first sheet and the second sheet.

Equation (4.1) contains a series that can be summed in closed form to give

$$pR_{\infty} = pr + \frac{ptpR_{\infty}pt}{1-prpR_{\infty}}$$

which results in the following quadratic equation for pR_{∞}

$$(pR_{\infty})^2 - \left(\frac{1-p^2(t^2-r^2)}{pr} \right) (pR_{\infty}) + 1 = 0 \quad (4.2)$$

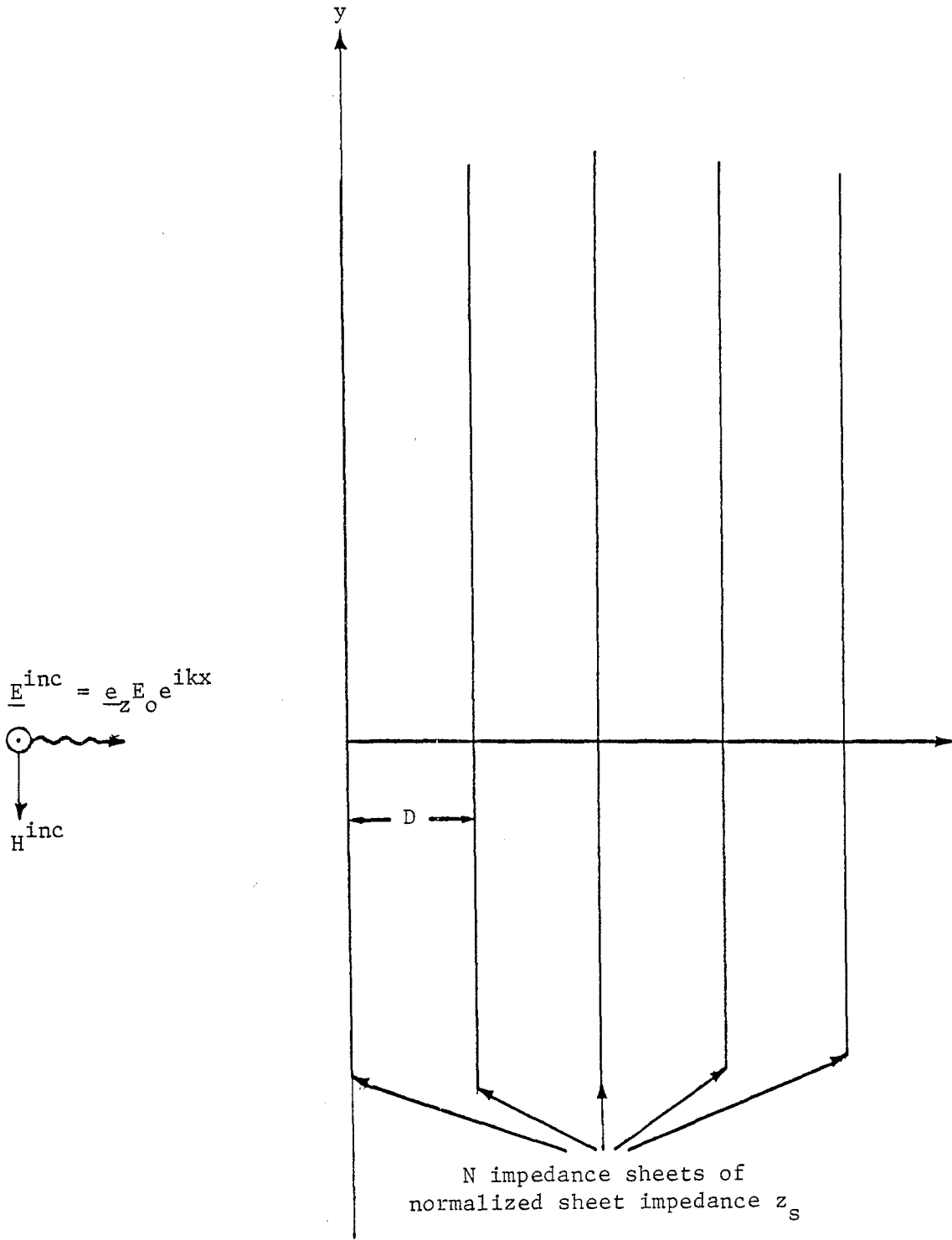


Figure 7. Several uniformly spaced impedance sheets.

But in Section III it was shown that the reflection coefficient of a single sheet is given by

$$r = -\frac{y_s}{2+y_s} \quad (4.3)$$

Thus

$$t = \frac{2}{2+y_s} \quad (4.4)$$

and

$$t^2 - r^2 = \frac{2-y_s}{2+y_s} \quad (4.5)$$

Substituting these expressions in equation (4.2), we obtain

$$(pR_\infty)^2 + \left(\frac{2}{y_s} \left(\frac{1}{p} - p \right) + \left(\frac{1}{p} + p \right) \right) pR_\infty + 1 = 0, \quad (4.6)$$

or substituting for p its value in terms of kD ($\equiv 2\pi D/\lambda$), we obtain

$$(pR_\infty)^2 + 2 \left(-\frac{2i}{y_s} \sin kD + \cos kD \right) pR_\infty + 1 = 0 \quad (4.7)$$

i.e., from equation (3.20)

$$(pR_\infty)^2 + 2 \left([-2iz_p + i(kdS_1 - 1)] \sin kD + \cos kD \right) pR_\infty + 1 = 0 \quad (4.8)$$

where z_p is the normalized post impedance ($\equiv Z_p/Z_0$).

If we neglect the discreteness contribution to z_s (the argument for doing this is given at the end of Section III), and use equation (2.10) for the post impedance (the argument for doing this is in Section II), equation (4.8) becomes

$$(pR_\infty)^2 + 2\left(\frac{2}{\alpha} \frac{\sin kD}{kD} + \cos kD\right)(pR_\infty) + 1 = 0 \quad (4.9)$$

where

$$\alpha \equiv \frac{A(\epsilon_r - 1)}{dD} \quad (4.10)$$

and A is the cross sectional area of a post. Note that α is the fractional increase in the average dielectric constant of the sheet medium (over the dielectric constant of free space), and so can be expected to be small in all cases of practical importance.

Now defining

$$F \equiv \left| \frac{2}{\alpha} \frac{\sin kD}{kD} + \cos kD \right|, \quad (4.11)$$

it is not difficult to show, from equation (4.9), that

$$\begin{aligned} |R_\infty| &= \left| F - \sqrt{F^2 - 1} \right| & F > 1 \\ &= 1 & F \leq 1 \end{aligned} \quad (4.12)$$

From equation (4.12) we have chosen to plot the present approximation to the percentage of the energy reflected from an infinite half space of impedance sheets as a function of $(2D/\lambda)$ with α as a parameter. This information is given in Table 3 and Figure 8.

Let us now turn to the determination of R_N , the reflection coefficient when only N impedance sheets are present. We expect R_N to approach the reflection coefficient we have calculated above as N approaches infinity, but we also expect R_N to have quite a different behavior when N is small (there will be no complete stop bands).

We will determine R_N by first calculating the sheets currents flowing in

Table 3. The percentage of energy reflected from an infinite number of sheets according to equation (4.12).

$(2D/\lambda)^\alpha$.01	.02	.04	.08	.16	.32
.05	.001	.002	.010	.037	.139	.485
.10	.001	.003	.010	.038	.143	.501
.15	.001	.003	.010	.040	.150	.529
.20	.001	.003	.011	.043	.160	.571
.25	.001	.003	.012	.046	.175	.631
.30	.001	.003	.013	.051	.196	.716
.35	.001	.004	.015	.058	.224	.835
.40	.001	.004	.017	.068	.263	1.004
.45	.001	.005	.020	.081	.318	1.253
.50	.002	.006	.025	.099	.398	1.631
.55	.002	.008	.031	.125	.517	2.239
.60	.002	.010	.040	.166	.705	3.297
.65	.003	.013	.055	.230	1.020	5.372
.70	.005	.019	.079	.340	1.604	10.403
.75	.007	.029	.123	.547	2.854	31.807
.80	.012	.049	.212	1.005	6.321	100.000
.85	.023	.097	.436	2.319	26.100	100.000
.90	.057	.252	1.258	9.437	100.000	100.000
.95	.279	1.421	11.695	100.000	100.000	100.000
1.00	100.000	100.000	100.000	100.000	100.000	100.000
1.05	.229	.777	2.320	5.941	12.715	22.902
1.10	.071	.257	.865	2.591	6.643	14.334
1.15	.037	.138	.491	1.587	4.505	10.951
1.20	.024	.093	.340	1.155	3.522	9.408
1.25	.019	.071	.267	.939	3.033	8.815
1.30	.015	.060	.228	.828	2.815	8.892
1.35	.014	.054	.209	.780	2.784	9.622
1.40	.013	.052	.203	.777	2.919	11.215
1.45	.013	.052	.208	.817	3.243	14.293
First 2 stop bands	.9901 } 1.0000 }	.9803 } 1.0000 }	.9615 } 1.0000 }	.9262 } 1.0000 }	.8639 } 1.0000 }	.7660 } 1.0000 }
	1.9802 } 2.0000 }	1.9608 } 2.0000 }	1.9234 } 2.0000 }	1.8543 } 2.0000 }	1.7378 } 2.0000 }	1.5739 } 2.0000 }

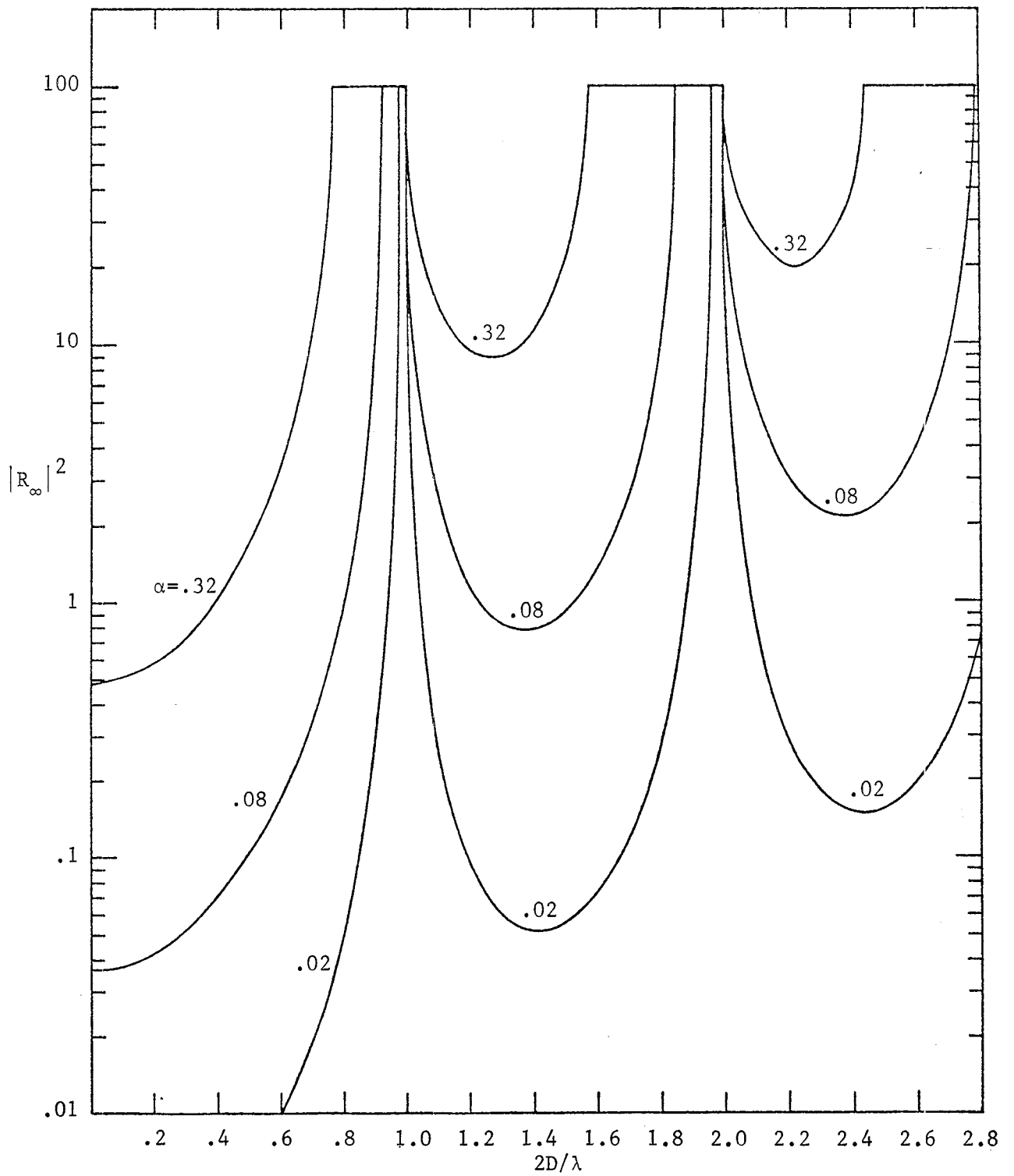


Figure 8. $|R_\infty|^2$ (in percent) vs. $(2D/\lambda)$ for various values of α for an infinite number of sheets.

each of the N sheets due to a normally incident plane wave and then computing the sum of the fields generated by the N sheet currents.

We know from equation (3.3) (or equation (3.16), by neglecting the evanescent modes) that the electric field due to the m^{th} sheet current (at position $x = (m - 1)D$) is given by

$$E_m = - \frac{Z_o K_m}{2} e^{ik|x-(m-1)D|} \quad (4.13)$$

at the position of the n^{th} sheet this gives

$$E_m^n = - \frac{Z_o K_m}{2} e^{ikD|n-m|} \quad (4.14)$$

Therefore the total electric field at the n^{th} sheet, i.e., the sum of the incident field and the fields radiated by all the sheet currents, is

$$E^n = E_o^{\text{inc}} e^{ikD(n-1)} - \frac{Z_o}{2} \sum_{m=1}^N K_m e^{ikD|n-m|} \quad n = 1, N \quad (4.15)$$

But we know that an alternative expression for E^n , from the definition of sheet impedance, is just $z_s^n Z_o K_n$, where z_s^n is the n^{th} normalized sheet impedance. Thus we can write the following set of equations for the sheet currents, K_m

$$z_s^n K_n + \frac{1}{2} \sum_{m=1}^N e^{ikD|n-m|} K_m = \frac{E_o^{\text{inc}}}{Z_o} e^{ikD(n-1)}, \quad n = 1, N \quad (4.16)$$

If all the sheet impedances are equal, i.e., $z_s^n = z_s = y_s^{-1}$, we can also write

$$K_n + \frac{y_s}{2} \sum_{m=1}^N e^{ikD|n-m|} K_m = \frac{y_s E_o^{\text{inc}}}{Z_o} e^{ikD(n-1)}, \quad n = 1, N \quad (4.17)$$

Once equations (4.17) have been solved for the K_m , we can use equation (4.13) to calculate the total field generated by all the sheet currents and thus determine the reflected field in the form

$$E^{\text{ref}} = -\frac{Z_0}{2} e^{-ikx} \sum_{m=1}^N K_m e^{i(m-1)kD}. \quad (4.18)$$

From equations (4.17) and (4.18) it easily follows that if we define normalized sheet currents by

$$x_m \equiv \frac{K_m Z_0}{E_0^{\text{inc}}} \quad (4.19)$$

then

$$R_N = -\frac{e^{-ikD}}{2} \sum_{m=1}^N x_m e^{imkD} \quad (4.20)$$

where

$$x_n + \frac{y_s}{2} \sum_{m=1}^N e^{ikD|n-m|} x_m = y_s e^{ikD(n-1)}, \quad n = 1, N \quad (4.21)$$

Equations (4.20) and (4.21) constitute our formulation of the N sheet reflection coefficient problem. Before we solve these equations completely, however, let us consider the possibility of a homogeneous solution for x_n when N is infinite and the sheets are uniformly distributed through all space. Such a solution will lead to the propagation and decay constants of waves propagating in the sheet medium, and, if the decay of such a wave is quite small in a length equivalent to the trestle of an ATLAS simulator, then even in "stop bands" there will be very little reflection from the finite length trestle. Thus, we will have a compact rough estimate of the effect of a trestle by displaying the propagation and decay constants in an infinite sheet medium. In order to calculate these constants, let us write equations (4.21) for such a medium in the form

$$x_n + \frac{y_s}{2} \sum_{m=-\infty}^{\infty} e^{ikD|n-m|} x_m = y_s e^{ikD(n-1)} \quad (4.22)$$

i.e.,

$$x_n + \frac{y_s}{2} \sum_{m=-\infty}^n e^{ikD(n-m)} x_m + \frac{y_s}{2} \sum_{m=n+1}^{\infty} e^{ikD(m-n)} x_m = y_s e^{ikD(n-1)} \quad (4.23)$$

and from this it follows that

$$x_{n+1} + \frac{y_s}{2} e^{ikD} \sum_{m=-\infty}^n e^{ikD(n-m)} x_m + \frac{y_s}{2} e^{-ikD} \sum_{m=n+1}^{\infty} e^{ikD(m-n)} x_m = y_s e^{ikDn} \quad (4.24)$$

$$\begin{aligned} x_{n-1} + (iy_s \sin kD)x_n + \frac{y_s}{2} e^{-ikD} \sum_{m=1}^n e^{ikD(n-m)} x_m \\ + \frac{y_s}{2} e^{ikD} \sum_{m=n+1}^{\infty} e^{ikD(m-n)} x_m = y_s e^{ikD(n-2)} \end{aligned} \quad (4.25)$$

Adding equations (4.24) and (4.25) and subtracting $2 \cos kD$ times equation (4.23) we obtain

$$x_{n+1} - 2(\cos kD - \frac{iy_s}{2} \sin kD)x_n + x_{n-1} = 0, \quad (4.26)$$

and this homogeneous equation is satisfied by a solution of the form

$$x_n = e^{in\theta} \quad (4.27)$$

where

$$\cos \theta = \cos kD - \frac{iy_s}{2} \sin kD. \quad (4.28)$$

Making the same approximations for y_s as we have made previously in this section, and using the definition of α in equation (4.10), equation (4.28) becomes

$$\theta = \theta_r + i\theta_i = \cos^{-1}[\cos kD - \frac{\alpha}{2} kD \sin kD]. \quad (4.29)$$

In table 4 and figures 9 and 10 we present values of $\theta_r - kD$ and θ_i calculated

Table 4a. Phase change per section of an infinite sheet medium.

$\alpha = .01$				$\alpha = .02$			
Pass Bands				Pass Bands			
$2D/\lambda$	$\theta_r - kD$	$2D/\lambda$	$\theta_r - kD$	$2D/\lambda$	$\theta_r - kD$	$2D/\lambda$	$\theta_r - kD$
.05	.00078	1.05	.01571	.05	.00156	1.05	.03013
.10	.00157	1.10	.01684	.10	.00313	1.10	.03290
.15	.00235	1.15	.01776	.15	.00469	1.15	.03494
.20	.00313	1.20	.01861	.20	.00626	1.20	.03678
.25	.00392	1.25	.01945	.25	.00782	1.25	.03854
.30	.00470	1.30	.02027	.30	.00939	1.30	.04026
.35	.00549	1.35	.02109	.35	.01097	1.35	.04198
.40	.00628	1.40	.02191	.40	.01254	1.40	.04369
.45	.00706	1.45	.02274	.45	.01412	1.45	.04541
.50	.00785	1.50	.02356	.50	.01571	1.50	.04714
.55	.00865	1.55	.02439	.55	.01730	1.55	.04890
.60	.00944	1.60	.02524	.60	.01891	1.60	.05071
.65	.01024	1.65	.02609	.65	.02053	1.65	.05256
.70	.01104	1.70	.02697	.70	.02217	1.70	.05451
.75	.01185	1.75	.02788	.75	.02385	1.75	.05661
.80	.01268	1.80	.02885	.80	.02559	1.80	.05898
.85	.01353	1.85	.02994	.85	.02745	1.85	.06192
.90	.01446	1.90	.03136	.90	.02963	1.90	.06655
.95	.01570	1.95	.03437	.95	.03337	1.95	.08319
1.00	.00000	2.00		1.00	.00000	2.00	

Stop Bands						Stop Bands					
$2D/\lambda$	θ_i										
.9900	.0000	.9935	.0148	.9970	.0144	.980	.0000	.987	.0294	.994	.0287
.9905	.0062	.9940	.0153	.9975	.0136	.981	.0107	.988	.0303	.995	.0271
.9910	.0090	.9945	.0155	.9980	.0126	.982	.0170	.989	.0309	.996	.0251
.9915	.0109	.9950	.0156	.9985	.0112	.983	.0211	.990	.0311	.997	.0224
.9920	.0123	.9955	.0156	.9990	.0094	.984	.0241	.991	.0310	.998	.0188
.9925	.0134	.9960	.0153	.9995	.0069	.985	.0264	.992	.0306	.999	.0137
.9930	.0142	.9965	.0149	1.0000	.0000	.986	.0281	.993	.0298	1.000	.0000

Table 4b. Phase change per section of an infinite sheet medium.

$\alpha = .04$				$\alpha = .08$			
Pass Bands				Pass Bands			
$2D/\lambda$	$\theta_r - kD$	$2D/\lambda$	$\theta_r - kD$	$2D/\lambda$	$\theta_r - kD$	$2D/\lambda$	$\theta_r - kD$
.05	.00311	1.05	.05608	.05	.00616	1.05	.10035
.10	.00622	1.10	.06304	.10	.01233	1.10	.11734
.15	.00934	1.15	.06780	.15	.01851	1.15	.12865
.20	.01246	1.20	.07190	.20	.02471	1.20	.13813
.25	.01559	1.25	.07574	.25	.03094	1.25	.14684
.30	.01872	1.30	.07947	.30	.03720	1.30	.15525
.35	.02187	1.35	.08316	.35	.04351	1.35	.16357
.40	.02503	1.40	.08685	.40	.04988	1.40	.17198
.45	.02822	1.45	.09058	.45	.05633	1.45	.18062
.50	.03142	1.50	.09439	.50	.06287	1.50	.18963
.55	.03466	1.55	.09831	.55	.06955	1.55	.19923
.60	.03794	1.60	.10241	.60	.07642	1.60	.20971
.65	.04129	1.65	.10678	.65	.08356	1.65	.22162
.70	.04472	1.70	.11156	.70	.09110	1.70	.23594
.75	.04831	1.75	.11707	.75	.09934	1.75	.25500
.80	.05216	1.80	.12398	.80	.10890	1.80	.28598
.85	.05658	1.85	.13432	.85	.12161	1.85	.38814
.90	.06262	1.90	.15874	.90	.14666	1.90	
.95	.07994	1.95		.95		1.95	
1.00	.00000	2.00		1.00	.00000	2.00	

Stop Band						Stop Band					
$2D/\lambda$	θ_i										
.960	.0000	.974	.0576	.988	.0571	.925	.0000	.950	.1128	.975	.1142
.962	.0128	.976	.0596	.990	.0540	.930	.0531	.955	.1177	.980	.1073
.964	.0299	.978	.0609	.992	.0500	.935	.0781	.960	.1202	.985	.0971
.966	.0393	.980	.0615	.994	.0447	.940	.0940	.965	.1205	.990	.0826
.968	.0459	.982	.0615	.996	.0376	.945	.1051	.970	.1185	.995	.0607
.970	.0509	.984	.0607	.998	.0274					1.000	.0000
.972	.0548	.986	.0593	1.000	.0000						

Table 4c. Phase change per section of an infinite sheet medium.

$\alpha = .16$				$\alpha = .32$							
Pass Bands				Pass Bands							
$2D/\lambda$	$\theta_r - kD$	$2D/\lambda$	$\theta_r - kD$	$2D/\lambda$	$\theta_r - kD$	$2D/\lambda$	$\theta_r - kD$				
.05	.01210	1.05	.17180	.05	.02341	1.05	.28204				
.10	.02423	1.10	.21024	.10	.04690	1.10	.36166				
.15	.03641	1.15	.23657	.15	.07057	1.15	.41984				
.20	.04866	1.20	.25868	.20	.09453	1.20	.47070				
.25	.06101	1.25	.27908	.25	.11889	1.25	.51946				
.30	.07350	1.30	.29894	.30	.14379	1.30	.56915				
.35	.08618	1.35	.31897	.35	.16944	1.35	.62245				
.40	.09910	1.40	.33978	.40	.19609	1.40	.68270				
.45	.11234	1.45	.36201	.45	.22411	1.45	.75563				
.50	.12600	1.50	.38655	.50	.25405	1.50	.85410				
.55	.14024	1.55	.41478	.55	.28685	1.55	1.02648				
.60	.15533	1.60	.44935	.60	.32416	1.60					
.65	.17170	1.65	.49628	.65	.36945	1.65					
.70	.19017	1.70	.57558	.70	.43186	1.70					
.75	.21261	1.75		.75	.55546	1.75					
.80	.24438	1.80		.80		1.80					
.85	.31611	1.85		.85		1.85					
Stop Bands						Stop Bands					
$2D/\lambda$	θ_i	$2D/\lambda$	θ_i	$2D/\lambda$	θ_i	$2D/\lambda$	θ_i	$2D/\lambda$	θ_i	$2D/\lambda$	θ_i
.860	.0000	.910	.2191	.960	.2111	.76	.0000	.85	.4094	.94	.3742
.865	.0416	.915	.2242	.965	.2025	.77	.1101	.86	.4186	.95	.3514
.870	.0958	.920	.2279	.970	.1921	.78	.2018	.87	.4244	.96	.3229
.875	.1267	.925	.2303	.975	.1794	.79	.2583	.88	.4271	.97	.2869
.880	.1495	.930	.2315	.980	.1641	.80	.3001	.89	.4267	.98	.2401
.885	.1675	.935	.2313	.985	.1451	.81	.3329	.90	.4231	.99	.1738
.890	.1822	.940	.2300	.990	.1209	.82	.3591	.91	.4163	1.00	.0000
.895	.1944	.945	.2273	.995	.0872	.83	.3801	.92	.4061		
.900	.2044	.950	.2233	1.000	.0000	.84	.3967	.93	.3922		
.905	.2126	.955	.2179								

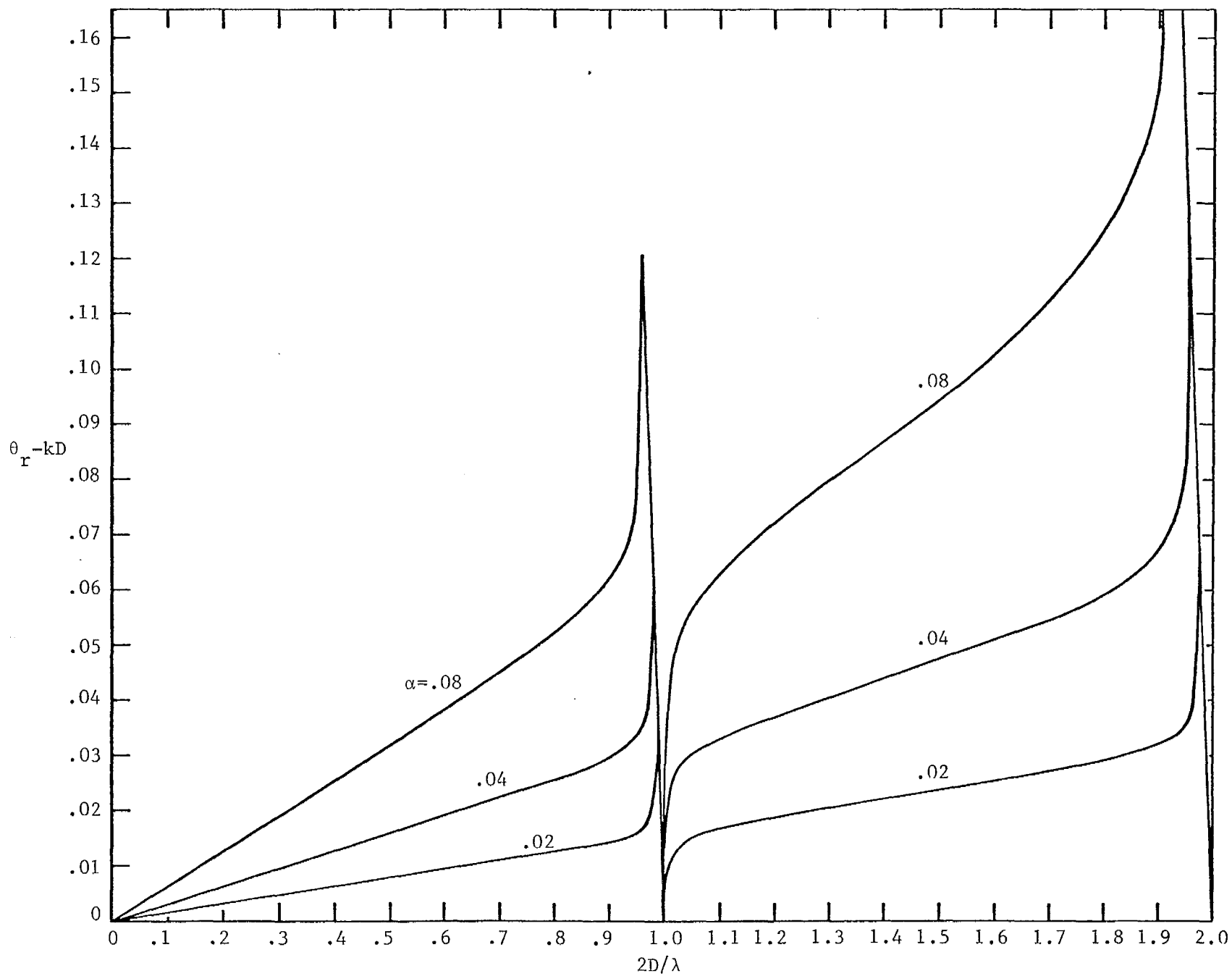


Figure 9. Phase change per section of a wave in an infinite sheet medium.

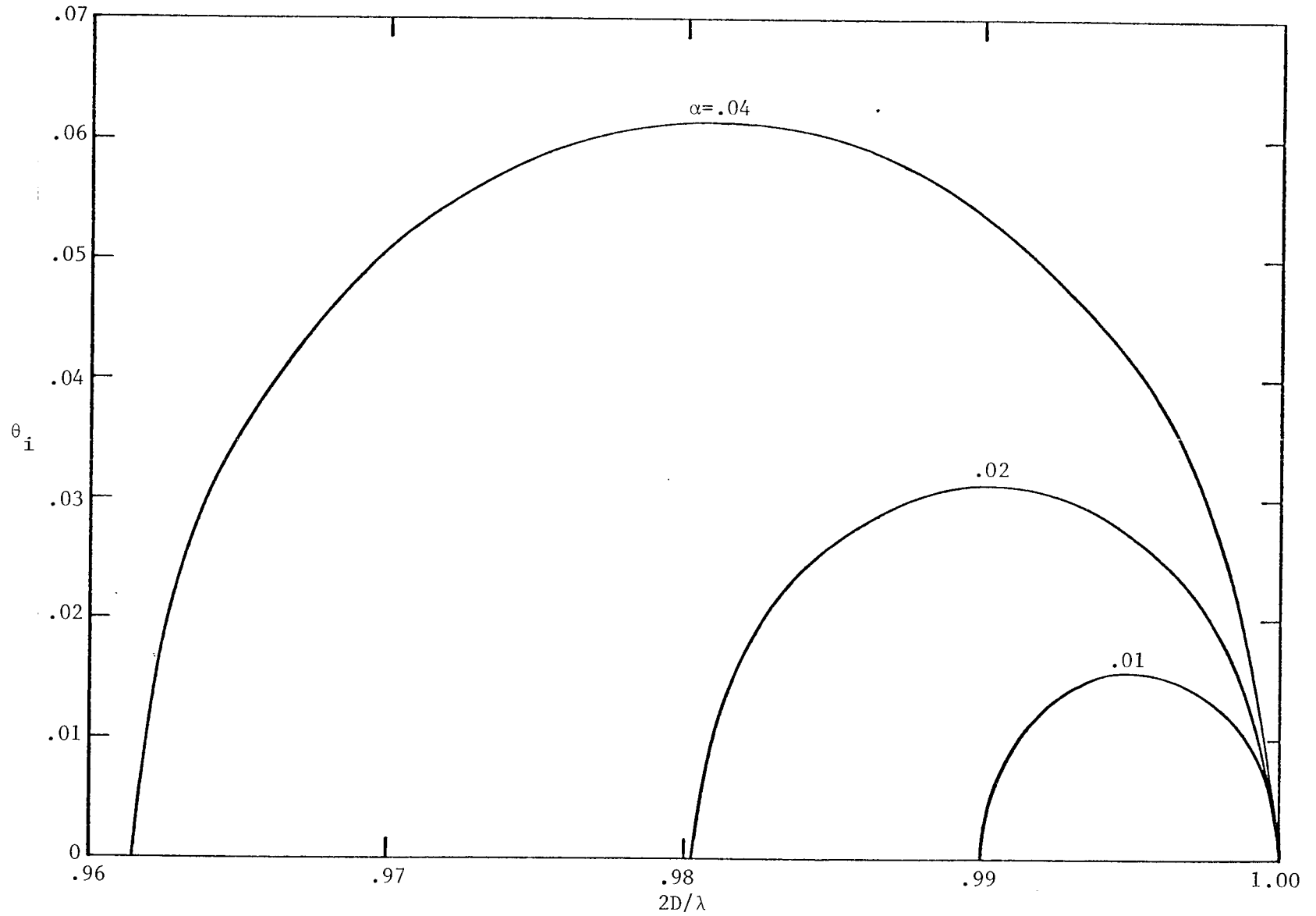


Figure 10. Decay constant per section in stop band of an infinite sheet medium.

from equation (4.29). We have used the same values of α as for table 3 and have taken kD through the first stop band. If there are N rows of posts in the real trestle, and $N\theta_{\perp}$ is small, for all kD in a stop band, there will be very little reflection even within the stop band. We note in passing that it is not difficult to show that for small values of α the maximum value of θ_{\perp} in the first stop band is about $(\alpha\pi/2)$, and this agrees quite well with the numerical data for α less than a tenth.

Turning now to the calculation of R_N from equations (4.20) and (4.21), it is shown in Appendix B that the solution of the set of equations

$$x_n + c \sum_{m=1}^N e^{ikD|n-m|} x_m = y_n, \quad n = 1, N \quad (4.30)$$

can be written in either of two equivalent forms. The first of these forms is

$$x_n = \sum_{m=1}^N G_{nm}^N (y_{m+1} - 2 \cos kDy_m + y_{m-1}) \quad (4.31)$$

where, by definition,

$$y_0 \equiv e^{ikD} y_1 \quad (4.32)$$

$$y_{N+1} \equiv e^{ikD} y_N \quad (4.33)$$

and the matrix G_{nm}^N is given explicitly by

$$G_{nm}^N = \frac{[e^{-ikD} \sin(N+1-m)\theta - \sin(N-m)\theta][e^{-ikD} \sin n\theta - \sin(n-1)\theta]}{\sin \theta e^{-ikD} [2 \sin N\theta - e^{ikD} \sin(N-1)\theta - e^{-ikD} \sin(N+1)\theta]} \quad n \leq m$$

$$= \frac{[e^{-ikD} \sin(N+1-n)\theta - \sin(N-n)\theta][e^{-ikD} \sin m\theta - \sin(m-1)\theta]}{\sin \theta e^{-ikD} [2 \sin N\theta - e^{ikD} \sin(N-1)\theta - e^{-ikD} \sin(N+1)\theta]} \quad n \geq m$$

(4.34)

where

$$\cos \theta \equiv \cos kD - ic \sin kD. \quad (4.35)$$

The second form of the solution of equations (4.30) is

$$x_n = y_n - 2ic \sin kD \sum_{p=1}^N G_{nm}^N y_m. \quad (4.36)$$

For c equal to $(y_s/2)$ and y_n equal to $y_s e^{ikD(n-1)}$, as we have in equation (4.21), equation (4.31) gives

$$x_n = 2iy_s \sin(kD) G_{n1}^N, \quad (4.37)$$

and θ is given by equation (4.28).

From equations (4.37) and (4.34) we thus have, as the solution to equations (4.21)

$$x_n = 2iy_s \sin kD \cdot \frac{e^{-ikD} \sin(N+1-n)\theta - \sin(N-n)\theta}{2 \sin N\theta - e^{ikD} \sin(N-1)\theta - e^{-ikD} \sin(N+1)\theta} \quad (4.38)$$

Using this expression, one could calculate R_N from equation (4.20), but is simpler to note that equation (4.21), written for $n = 1$, is just

$$x_1 - y_s R_N = y_s. \quad (4.39)$$

Thus

$$R_N = -1 + x_1/y_s, \quad (4.40)$$

or, using equation (4.38),

$$R_N = 2i \sin kD \cdot \frac{e^{-ikD} \sin N\theta - \sin(N-1)\theta}{2 \sin N\theta - e^{ikD} \sin(N-1)\theta - e^{-ikD} \sin(N+1)\theta} - 1. \quad (4.41)$$

Algebraic simplification reduces equation (4.41) to

$$R_N = \frac{(1 - e^{2iN\theta}) R_\infty}{1 - e^{2i(kD + N\theta)} R_\infty^2}, \quad (4.42)$$

where

$$R_\infty \equiv - \frac{e^{-ikD} e^{-i\theta}}{e^{ikD} e^{-i\theta}} \quad (4.43)$$

is the reflection coefficient when N is infinite.

It can be shown that expression (4.43), with θ given by equation (4.29) is identical to the R_∞ given by the solution to quadratic equation (4.7). It can also be shown that equation (4.42), for $N = 1$, reduces quite nicely to the reflection coefficient of equation (4.3). These mathematical manipulations will not be presented here, but those readers interested in that sort of thing should have little difficulty in performing them.

Special simplifications occur in equation (4.42) if y_s is assumed to be pure imaginary. In particular if we approximate y_s , as we have done before, by $(-ikD_0)$, then θ is given by equation (4.29) and so is either purely real (pass bands) or of the form $n\pi + i\theta_i$ (stop bands). Let us examine these cases individually. In the case of a pass band we have

$$|R_N|^2 = \frac{\left(1 - e^{2iN\theta_r}\right) \left(1 - e^{-2iN\theta_r}\right) |R_\infty|^2}{1 - e^{2iN\theta_r} e^{2ikD} |R_\infty|^2} \quad (4.44)$$

$$= \frac{4 \sin^2 N\theta_r |R_\infty|^2}{1 + |R_\infty|^4 - 2R_\infty^2 e^{2ikD} e^{2iN\theta_r} - R_\infty^{*2} e^{-2ikD} e^{-2iN\theta_r}} \quad (4.45)$$

But from the alternative expression for R_∞ implied by equation (4.9) it is clear that in a pass band $e^{ikD} R_\infty$ is real. Thus we can write

$$|R_N|^2 = \frac{4 \sin^2 N\theta_r |R_\infty|^2}{1 + |R_\infty|^4 - 2R_\infty^2 e^{2ikD} \cos 2N\theta_r} \quad (4.46)$$

Again, since $e^{ikD} R_\infty$ is real, we can write $e^{2ikD} R_\infty^2 = |R_\infty|^2$ and so obtain

$$\begin{aligned}
 |R_N|^2 &= \frac{4 \sin^2 N\theta_r |R_\infty|^2}{1 + |R_\infty|^4 - 2|R_\infty|^2 \cos 2N\theta_r} \\
 &= \frac{4 \sin^2 N\theta_r |R_\infty|^2}{(1 - |R_\infty|^2)^2 + 4|R_\infty|^2 \sin^2 N\theta_r} \\
 &= \sin^2 N\theta_r \left\{ \frac{(1 - |R_\infty|^2)^2}{4|R_\infty|^2} + \sin^2 N\theta_r \right\}^{-1}
 \end{aligned} \tag{4.47}$$

But, using expression (4.12) it is not hard to show that

$$\frac{(1 - |R_\infty|^2)^2}{4|R_\infty|^2} = F^2 - 1 \tag{4.48}$$

Thus from equations (4.47) and (4.48) we have, in a pass band of an N sheet structure whose y_s is $-ikD\alpha$,

$$|R_N|^2 = \frac{\sin^2 N\theta_r}{\sin^2 N\theta_r + F^2 - 1} \tag{4.49}$$

where θ_r is given by equation (4.29) and F is given by equation (4.11).

Similar considerations lead us to the conclusion that, in a stop band of an N sheet structure whose y_s is $-ikD\alpha$,

$$|R_N|^2 = \frac{\sinh^2 N\theta_i}{\sinh^2 N\theta_i + 1 - F^2} \tag{4.50}$$

where again θ_i is given by equation (4.29) and F is given by equation (4.11).

We have chosen to display the data on $|R_N|^2$ in the form of linear plots of $|R_N|$ against $2D/\lambda$ with α and N as parameters. Figures 11, 12, 13, and 14 contain this information for N values of 1, 2, 4, and 8 respectively. From the definition of α , the lower α values shown are in the range to be expected of any trestle structure that fulfills its electromagnetic purpose. Some of the $|R_N|$ data is also given in tabular form in table 5.

The following curves and tables are perhaps the most relevant numerical information in this note for purposes of trestle analysis. In Section V we will get an idea of how close these $|R_N|$ values are to the values that would be calculated if the discreteness of the sheets were kept in consideration and if evanescent mode interactions were also retained.

In closing this section we can note the form that some of the results take for very small α values. It follows from equation (4.29) that if $(2D/\lambda)$ is not too close to unity we can write, for small α ,

$$\theta_r - kD \approx \frac{\alpha\pi}{2} (2D/\lambda), \quad (4.51)$$

while within the first stop band we have

$$\theta_i \approx \pi\sqrt{\delta(\alpha - \delta)}, \quad (4.52)$$

where

$$\delta \equiv 1 - (2D/\lambda). \quad (4.53)$$

If equation (4.52) is substituted in equation (4.50), and $N\theta_i$ is small, we have the approximate $|R_N|$ for small α in the first stop band as

$$|R_N| \approx \frac{N\pi\alpha}{2}. \quad (4.54)$$

The $|R_N|$ in the first pass band would be less than that given by equation (4.54).

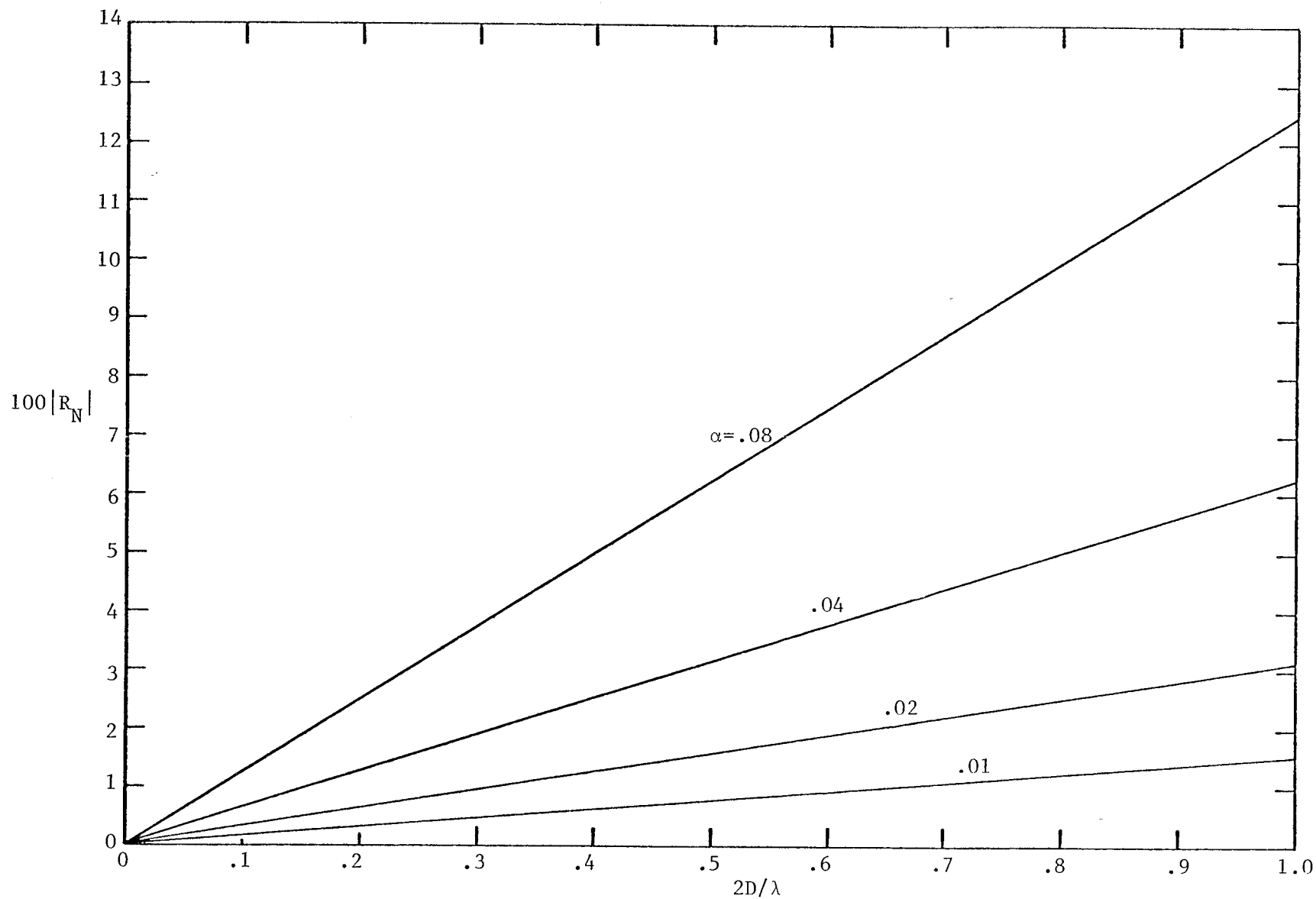


Figure 11. $100|R_N|$ vs. $2D/\lambda$ for $N = 1$ and various α .

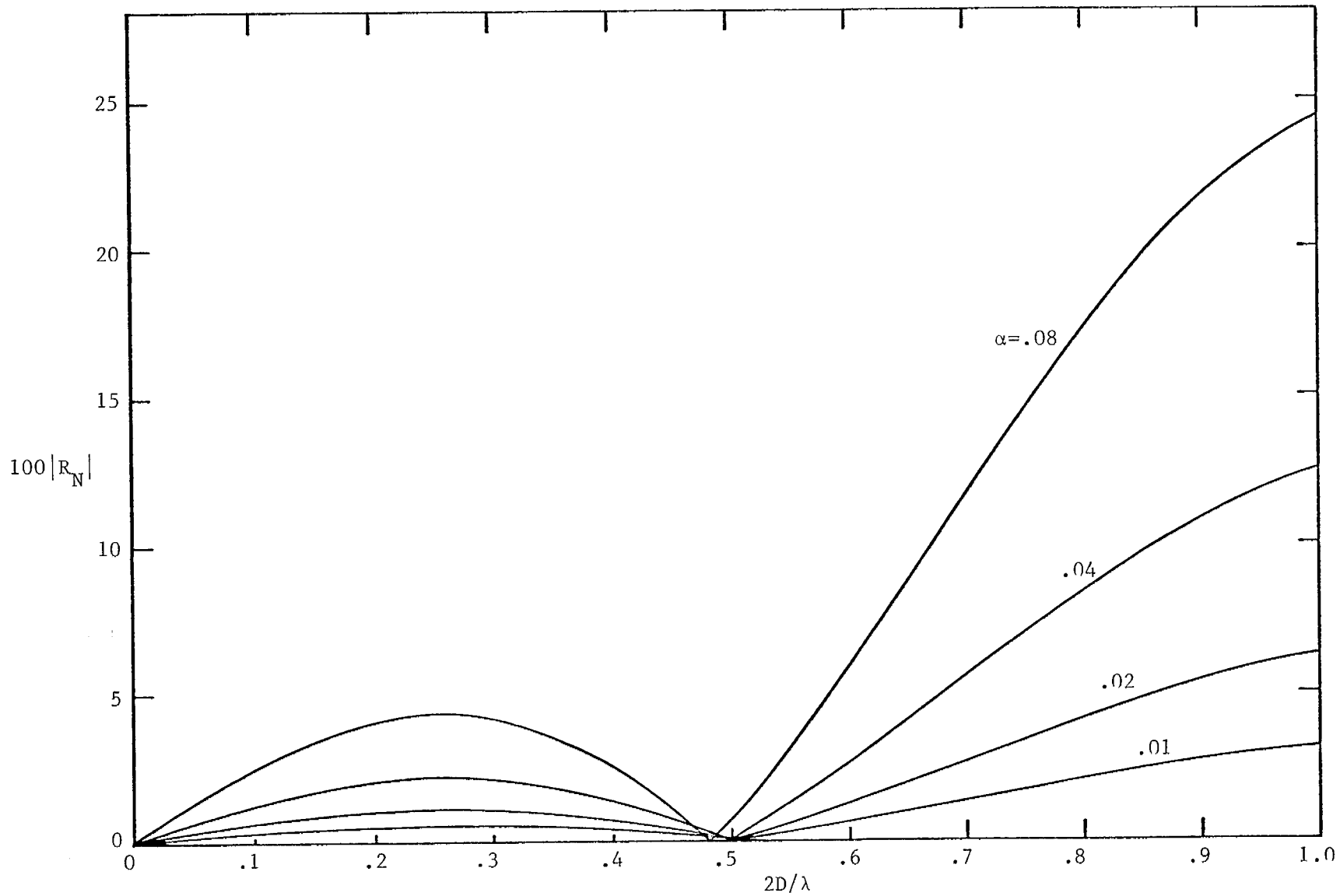


Figure 12. $100|R_N|$ vs. $2D/\lambda$ for $N = 2$ and various α .

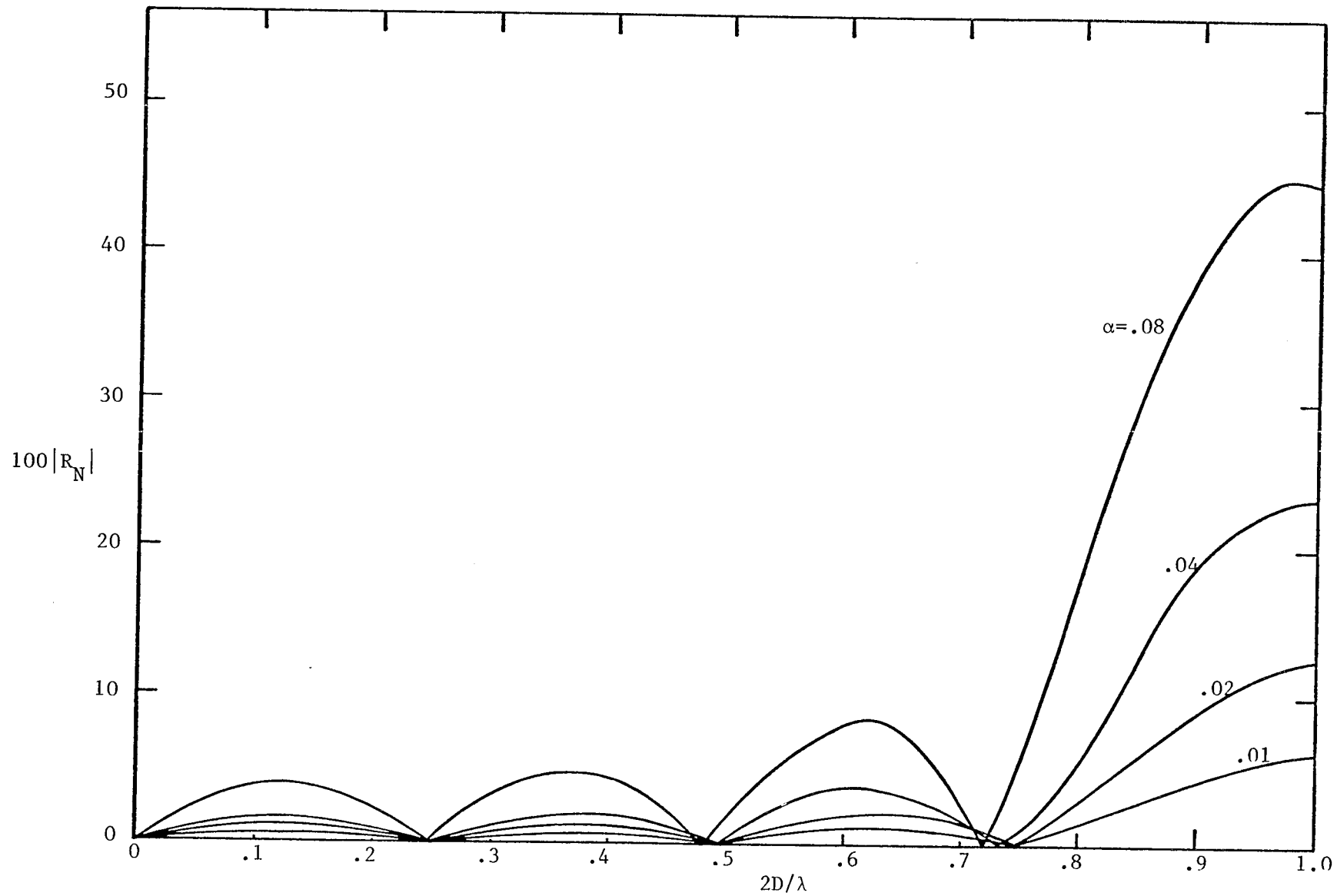


Figure 13. $100|R_N|$ vs. $2D/\lambda$ for $N = 4$ and various α .

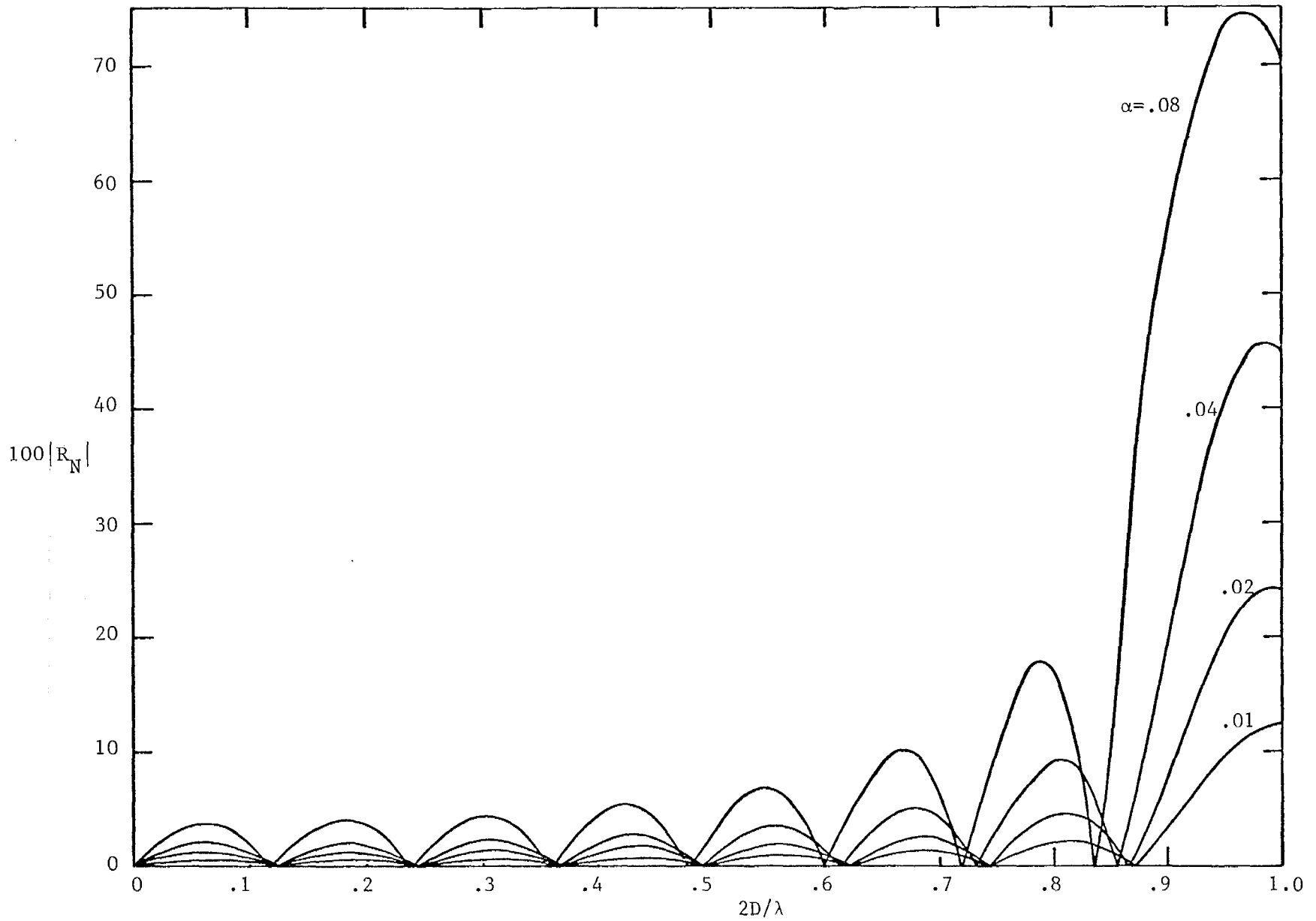


Figure 14. $100|R_N|$ vs. $2D/\lambda$ for $N = 8$ and various α .

Table 5a. $100|R_N|$ vs. $2D/\lambda$ for $\alpha = .01$ and various N .

$2D/\lambda$	N	1	2	4	8	16
.04		.063	.125	.241	.423	.449
.08		.126	.243	.426	.453	.394
.12		.188	.350	.509	.056	.112
.16		.251	.440	.468	.407	.506
.20		.314	.507	.307	.502	.334
.24		.377	.548	.061	.120	.235
.28		.440	.558	.219	.404	.569
.32		.503	.534	.465	.578	.262
.36		.565	.476	.615	.203	.384
.40		.628	.381	.622	.414	.644
.44		.691	.250	.467	.698	.164
.48		.754	.083	.166	.323	.584
.52		.817	.116	.229	.441	.743
.56		.880	.345	.637	.897	.014
.60		.942	.599	.956	.522	.888
.64		1.005	.874	1.087	.493	.885
.68		1.068	1.164	.946	1.267	.260
.72		1.131	1.461	.482	.912	1.438
.76		1.194	1.760	.305	.602	1.131
.80		1.257	2.051	1.367	2.127	.898
.84		1.319	2.329	2.599	1.960	2.805
.88		1.382	2.584	3.863	.919	1.786
.92		1.445	2.809	4.997	5.845	3.689
.96		1.508	2.997	5.842	10.540	13.441
1.00		1.571	3.140	6.271	12.468	24.375

Table 5b. $100|R_N|$ vs. $2D/\lambda$ for $\alpha = .02$ and various N.

$2D/\lambda$	N	1	2	4	8	16
.04		.126	.249	.483	.844	.890
.08		.251	.487	.850	.897	.796
.12		.377	.700	1.013	.097	.193
.16		.503	.878	.927	.822	.997
.20		.628	1.012	.601	.990	.706
.24		.754	1.091	.104	.208	.408
.28		.880	1.109	.454	.832	1.130
.32		1.005	1.060	.941	1.141	.606
.36		1.131	.940	1.231	.352	.675
.40		1.257	.747	1.230	.876	1.307
.44		1.382	.480	.903	1.383	.477
.48		1.508	.144	.287	.563	1.045
.52		1.633	.258	.510	.970	1.563
.56		1.759	.720	1.319	1.792	.280
.60		1.885	1.232	1.938	.916	1.627
.64		2.010	1.785	2.163	1.151	1.976
.68		2.136	2.366	1.829	2.565	.084
.72		2.261	2.961	.843	1.618	2.722
.76		2.387	3.557	.790	1.541	2.781
.80		2.512	4.137	2.957	4.403	.963
.84		2.638	4.687	5.441	3.546	5.583
.88		2.764	5.190	7.948	2.816	5.275
.92		2.889	5.632	10.148	12.855	4.988
.96		3.015	5.996	11.736	21.577	31.403
1.00		3.140	6.271	12.468	24.375	44.991

Table 5c. $100|R_N|$ vs. $2D/\lambda$ for $\alpha = .04$ and various N .

$2D/\lambda$	N	1	2	4	8	16
.04		.251	.499	.964	1.681	1.744
.08		.503	.972	1.695	1.759	1.623
.12		.754	1.398	2.009	.132	.264
.16		1.005	1.752	1.818	1.678	1.927
.20		1.257	2.014	1.149	1.924	1.548
.24		1.508	2.167	.143	.285	.564
.28		1.759	2.195	.973	1.754	2.198
.32		2.010	2.086	1.926	2.210	1.509
.36		2.261	1.833	2.462	.484	.950
.40		2.512	1.433	2.400	1.932	2.611
.44		2.764	.886	1.681	2.688	1.504
.48		3.015	.197	.394	.780	1.507
.52		3.266	.623	1.224	2.271	3.278
.56		3.516	1.562	2.815	3.520	1.535
.60		3.767	2.599	3.960	1.282	2.429
.64		4.018	3.714	4.254	2.927	4.467
.68		4.269	4.881	3.378	5.137	1.620
.72		4.519	6.071	1.169	2.294	4.249
.76		4.770	7.255	2.331	4.419	7.058
.80		5.020	8.400	6.836	9.139	1.889
.84		5.271	9.476	11.838	5.135	9.286
.88		5.521	10.449	16.689	10.026	16.359
.92		5.771	11.219	20.732	29.883	5.730
.96		6.021	11.973	23.418	43.219	68.438
1.00		6.271	12.468	24.375	44.991	70.898

Table 5d. $100|R_N|$ vs. $2D/\lambda$ for $\alpha = .08$ and various N.

$2D/\lambda$	N	1	2	4	8	16
.04		.503	.997	1.926	3.336	3.350
.08		1.005	1.942	3.365	3.379	3.351
.12		1.508	2.786	3.946	.029	.057
.16		2.010	3.483	3.497	3.468	3.525
.20		2.512	3.989	2.089	3.604	3.531
.24		3.015	4.269	.029	.059	.118
.28		3.516	4.291	2.190	3.809	3.911
.32		4.018	4.033	4.003	4.063	3.940
.36		4.519	3.480	4.895	.092	.184
.40		5.020	2.625	4.531	4.453	4.604
.44		5.521	1.471	2.838	4.882	4.708
.48		6.021	.031	.063	.125	.250
.52		6.521	1.673	3.235	5.629	5.825
.56		7.020	3.608	6.258	6.361	6.150
.60		7.518	5.732	8.127	.138	.276
.64		8.017	7.993	8.039	7.947	8.129
.68		8.514	10.335	5.410	9.322	9.195
.72		9.011	12.693	.002	.005	.009
.76		9.507	15.001	7.925	13.590	13.287
.80		10.003	17.194	17.435	16.943	17.884
.84		10.497	19.209	27.103	1.950	3.889
.88		10.991	20.986	35.469	39.210	29.990
.92		11.485	22.471	41.512	65.805	82.466
.96		11.977	23.615	44.732	74.752	95.829
1.00		12.468	24.375	44.911	70.898	89.537

V. Reflection From Several Rows of Posts -- a More General Approach

In this section we will outline a more general and more accurate approach to the calculation of the reflection from several rows of posts than the effective sheet impedance method of the previous section. We will still assume that the incident wave is normally incident on the rows, and this implies that the equivalent currents are the same in all the posts of any given row. Thus, if the equivalent current in any post of the n^{th} row is I_n , if all post impedances are Y_p , and if the transverse post spacing is d while the longitudinal post spacing is D , it is clear from equations (2.6) and the definition of Y_p that

$$I_n = Y_p \left\{ E_o^{\text{inc}} e^{ikD(n-1)} - \frac{\omega\mu}{4} \sum_{m=1}^N I_m \sum_{j=-\infty}^{\infty} H_o^{(1)} \left(\sqrt{k^2 d^2 + (n-m)^2 D^2} \right) \right\} \quad (5.1)$$

where the prime on the inner summation means that the term where $n = m$ and $j = 0$ is omitted. Using previously developed transformations of the Hankel function sum ([22] or Section III), and defining

$$x_n \equiv \frac{Z_o I_n}{d E_o^{\text{inc}}}$$

$$y_s^o \equiv \frac{Y_p}{Y_d},$$

we may rewrite equation (5.1) as

$$x_n + \frac{y_s^o}{2} \sum_{m=1}^N e^{ikD|n-m|} x_m = y_s^o e^{ikD(n-1)} + \frac{y_s^o}{2} \sum_{m=1}^N P_{n-m} x_m \quad (5.2)$$

where

$$P_o = \frac{d}{\lambda} \left\{ \pi + 2i \left[\gamma + \ln\left(\frac{d}{2\lambda}\right) + \sum_{n=1}^{\infty} \left(\frac{1}{\sqrt{n^2 - (d/\lambda)^2}} - \frac{1}{n} \right) \right] \right\} \quad (5.3)$$

$$P_n = 2i \sum_{m=1}^{\infty} \frac{e^{-nkD\sqrt{(m\lambda/d)^2 - 1}}}{\sqrt{(m\lambda/d)^2 - 1}} \quad (5.4)$$

When equations (5.2) have been solved for the x_n , the reflection coefficient, R_N , can be found from equation (4.20).

The first thing to notice about equations (5.2) is that, when $[(y_s^0/2)P_{n-m}]$ is neglected in comparison with $[\delta_{nm} + (y_s^0/2)e^{ikD|n-m|}]$, equations (5.2) reduce to equations (4.21) if the discreteness contribution to y_s is neglected (and this is what we did in computing the numerical results of Section IV).

The next thing to notice about equations (5.2) is that if one keeps the P_0 term but neglects all other P_n terms (it is clear that if d/λ is small P_0 will really be much the largest of the P_n 's), and rearranges equations (5.2) appropriately, the result is the set (4.21) with y_s being now given by equation (3.19).

The third thing to notice is that if very accurate solutions of the multiple post problem were desired, a numerical solution to equations (5.2), as they stand, could be effected. We believe the other approximations we have made in going from the actual trestle reflection problem to equations (5.2) justify our slightly further approximation to equations (4.21), which possess an analytical solution. To test the accuracy of the step from equations (5.2) to equations (4.21) we will use equations (5.2) to calculate the phase change per row of posts in an infinite post medium. A comparison between this phase change and that of table 4 (Section IV) will give an idea of the accuracy to be expected from the other numerical results of Section IV.

To calculate the phase change per row of posts in an infinite medium we assume that n and m may go from minus infinity to plus infinity in equation (5.2) and substitute $x_n = e^{in\theta}$, with the forcing term being set to zero. The result is

$$e^{in\theta} + \frac{y_s^0}{2} \sum_{m=-\infty}^{\infty} e^{ikD|n-m|} e^{im\theta} = \frac{y_s^0}{2} \sum_{m=-\infty}^{\infty} P_{n-m} e^{im\theta} \quad (5.5)$$

or, relabelling indices,

$$e^{in\theta} + \frac{y_s^0}{2} \sum_{p=-\infty}^{\infty} e^{ikD|p|} e^{in\theta} e^{ip\theta} = \frac{y_s^0}{2} \sum_{p=-\infty}^{\infty} P_p e^{in\theta} e^{ip\theta} \quad (5.6)$$

$$1 + \frac{y_s^0}{2} \sum_{p=-\infty}^{\infty} e^{ikD|p|} e^{ip\theta} = \frac{y_s^0}{2} \sum_{p=-\infty}^{\infty} P_p e^{ip\theta} \quad (5.7)$$

Assuming k to be complex (with a positive imaginary part), temporarily, in order to get convergent sums, and then letting the imaginary part of k approach zero, we get

$$1 - \frac{iy_s^0}{2} \frac{\sin kD}{\cos kD - \cos \theta} = \frac{y_s^0}{2} \left\{ P_0(d/\lambda) + \frac{id}{\lambda} \sum_{n=1}^{\infty} \frac{1}{\sqrt{n^2 - (d/\lambda)^2}} \cdot \frac{\cos \theta - e^{-(2\pi D/d)\sqrt{n^2 - (d/\lambda)^2}}}{\cosh(2\pi D/d)\sqrt{n^2 - (d/\lambda)^2} - \cos \theta} \right\} \quad (5.8)$$

or, in terms of the parameters we have previously used, i.e., substituting

$$y_s^0 = -i(kD)\alpha \quad (5.9)$$

$$kD \equiv \pi x \quad (5.10)$$

$$d/2D \equiv r \quad (5.11)$$

we can write

$$1 - \frac{\pi x \alpha}{2} \cdot \frac{\sin \pi x}{\cos \pi x - \cos \theta} = -i\pi \alpha r x^2 \left\{ \frac{\pi}{2} + i \left[\gamma + \ln\left(\frac{xr}{2}\right) + \sum_{n=1}^{\infty} \left(\frac{1}{\sqrt{n^2 - (xr)^2}} - \frac{1}{n} \right) \right] \right\} + \frac{\pi \alpha r x^2}{2} \sum_{n=1}^{\infty} \frac{1}{\sqrt{n^2 - (xr)^2}} \cdot \frac{\cos \theta - e^{-(\pi/r)\sqrt{n^2 - (xr)^2}}}{\cosh(\pi/r)\sqrt{n^2 - (xr)^2} - \cos \theta} \quad (5.12)$$

For small r the right hand side of this equation approaches zero and we return to equation (4.28). But even for r not so small, the right hand side doesn't have too much effect on the θ roots of the above equation, as we can see by comparing table 6 (the solution of equation (5.12)) with table 4.

Table 6a. Phase change per row of an infinite post medium.

$\alpha = .01$						
$2D/\lambda$	$r = .1$		$r = .2$		$r = .4$	
	$\theta_r - kD$	$\theta_i \times 10^4$	$\theta_r - kD$	$\theta_i \times 10^4$	$\theta_r - kD$	$\theta_i \times 10^4$
.05	.00078	.0001	.00078	.0002	.00078	.0004
.10	.00157	.0008	.00157	.0015	.00157	.0031
.15	.00235	.0026	.00235	.0052	.00235	.0104
.20	.00313	.0062	.00313	.0123	.00313	.0247
.25	.00391	.0121	.00391	.0241	.00390	.0479
.30	.00469	.0209	.00469	.0415	.00468	.0825
.35	.00544	.0330	.00544	.0657	.00544	.1307
.40	.00628	.0492	.00627	.0980	.00626	.1945
.45	.00703	.0700	.00700	.1393	.00698	.2760
.50	.00778	.0960	.00775	.1908	.00770	.3773
.55	.00862	.1278	.00857	.2535	.00852	.5004
.60	.00934	.1659	.00929	.3287	.00924	.6474
.65	.01016	.2109	.01011	.4174	.01006	.8203
.70	.01090	.2637	.01085	.5209	.01079	1.0215
.75	.01163	.3248	.01157	.6408	.01151	1.2536
.80	.01248	.3955	.01240	.7790	.01233	1.5201
.85	.01322	.4776	.01313	.9391	.01305	1.8278
.90	.01416	.5760	.01406	1.1303	.01397	2.1938
.95	.01547	.7159	.01529	1.4014	.01509	2.7099

Table 6b. Phase change per row of an infinite post medium.

$\alpha = .02$

2D/ λ	r = .1		r = .2		r = .4	
	$\theta_r - kD$	$\theta_i \times 10^4$	$\theta_r - kD$	$\theta_i \times 10^4$	$\theta_r - kD$	$\theta_i \times 10^4$
.05	.00156	.0004	.00156	.0008	.00156	.0015
.10	.00313	.0031	.00313	.0061	.00312	.0123
.15	.00469	.0104	.00469	.0207	.00468	.0415
.20	.00625	.0246	.00625	.0489	.00622	.0974
.25	.00780	.0478	.00779	.0953	.00776	.1893
.30	.00936	.0826	.00934	.1643	.00929	.3255
.35	.01092	.1310	.01088	.2601	.01081	.5140
.40	.01248	.1953	.01241	.3871	.01232	.7626
.45	.01404	.2778	.01394	.5495	.01381	1.0787
.50	.01560	.3808	.01546	.7514	.01529	1.4697
.55	.01716	.5065	.01699	.9970	.01676	1.9427
.60	.01872	.6574	.01850	1.2908	.01822	2.5047
.65	.02028	.8362	.02002	1.6373	.01968	3.1634
.70	.02184	1.0460	.02154	2.0420	.02113	3.9277
.75	.02340	1.2910	.02309	2.5124	.02258	4.8094
.80	.02505	1.5776	.02467	3.0599	.02407	5.8284
.85	.02680	1.9194	.02634	3.7093	.02563	7.0273
.90	.02884	2.3573	.02829	4.5360	.02744	8.5398
.95	.03231	3.1580	.03158	6.0319	.03048	11.234

Table 6c. Phase change per row of an infinite post medium.

$\alpha = .04$

2D/ λ	r = .1		r = .2		r = .4	
	$\theta_r - kD$	$\theta_i \times 10^4$	$\theta_r - kD$	$\theta_i \times 10^4$	$\theta_r - kD$	$\theta_i \times 10^4$
.05	.00311	.0015	.00311	.0030	.00311	.0061
.10	.00622	.0122	.00621	.0243	.00620	.0487
.15	.00932	.0411	.00930	.0816	.00928	.1624
.20	.01242	.0969	.01239	.1928	.01233	.3822
.25	.01551	.1890	.01545	.3750	.01535	.7401
.30	.01859	.3259	.01849	.6448	.01832	1.2661
.35	.02167	.5164	.02150	1.0183	.02126	1.9885
.40	.02474	.7692	.02452	1.5111	.02415	2.9330
.45	.02781	1.0931	.02749	2.1385	.02700	4.1232
.50	.03087	1.4969	.03046	2.9154	.02980	5.5814
.55	.03394	1.9900	.03340	3.8571	.03255	7.3288
.60	.03701	2.5826	.03634	4.9801	.03527	9.3877
.65	.04014	3.2870	.03929	6.3037	.03796	11.784
.70	.04326	4.1192	.04229	7.8533	.04064	14.552
.75	.04652	5.1036	.04527	9.6692	.04334	17.750
.80	.04997	6.2866	.04846	11.829	.04616	21.497
.85	.05387	7.7810	.05204	14.524	.04928	26.095
.90	.05915	10.005	.05684	18.469	.05341	32.667
.95	.07357	17.831	.06955	31.484	.06390	52.528

VI. Concluding Remarks

The analysis presented in this note has been sufficient to put some fairly good bounds on the amount of reflection that a trestle support structure will cause. One simply assumes all the wood of the trestle to be in sheets, perpendicular to the incident wave and having the same periodicity as the real trestle in the direction of propagation of the incident wave. A bound on the reflected energy can then be found from the tables and curves of Section IV.

Should more accurate calculations be found necessary at some future time, there are many ways in which the work of the present note could be extended. Ten of these, in approximate order of increasing difficulty are as follows:

1. It would not be a very difficult matter to extend the work of the present note, which considered only normally incident waves, to the case where the incident wave arrives at some arbitrary angle. The generalized sum transformation formulas exist (in [22] for example). The easiest generalization would be to the case where the incident wave propagation vector is still perpendicular to the posts but not perpendicular to the rows of posts. However, the more general case could also be handled.
2. It would be fairly easy to extend the work of Appendix A to the point where numerical values for reflection coefficients of the other polarization could be computed. This polarization is not as important in reflecting waves, but the calculation would have some use if the bounds discussed at the beginning of this section should prove too rough.
3. One could readily extend the frequency range, somewhat, of the calculations presented here. We have limited the computations here, for the most part, to frequency values through the first stop band. A little care should be taken in invoking the sum transformation formulas at wavelengths close to the transverse post spacing. Otherwise no difficulty should be encountered. The extension of the frequency range

imagined here should not be such that there is more than the TEM propagating mode within the post medium. Thus we can still restrict ourselves, with good accuracy, to considering only TEM interactions among sheets with a modified y_s .

4. At frequencies higher than those that can be handled by extension 3, one could still calculate reflection coefficients by numerically solving equation (5.2). This would be necessary at frequencies high enough that non-TEM propagating modes could exist (i.e., $\lambda < d$).
5. For very thick posts, or at higher frequencies, it may be necessary to take into account higher order terms in the series (2.4). This would complicate the whole analysis somewhat, but it could still be carried through in a straightforward manner.
6. If it is necessary to take into account more than one post direction, for example alternate rows of horizontal and vertical posts, the analysis could be carried out by allowing for spatially varying equivalent currents in the posts. The currents could be assumed to be Fourier series in the variable along their length, the fundamental period of the Fourier series being the distance along their length between posts of the perpendicular rows.
7. If it is necessary to take into account the finite width of the actual trestle post arrays, the simplification of equal equivalent currents in each post becomes impossible. In this case the number of simultaneous equations to be solved in order to determine the post equivalent currents increases tremendously, but, if there are less than a hundred posts altogether the problem could still be readily handled numerically.
8. If the finite length of the posts is also to be treated the problem becomes just as complicated as that of calculating the reflection from several dozen wires. There is no difficulty in principle, but

the necessary computer times could well be prohibitive.

9. The effect of the interconnections between the posts would be a further complication of the finite length post problem. Techniques exist for handling crossed wire problems. Presumably they could be taken over and applied to the crossed "dielectric wire" problem.
10. For larger posts at higher frequencies it may be necessary to use one of the integral equation techniques mentioned in Section II to calculate the modal coefficients for extension 5 above. The development of a computer program to solve equations (2.14) and (2.15), for example, would be a time consuming project.

Appendix A

The Other Polarization

In this appendix we will give arguments for neglecting any incident wave polarization other than the one considered in the main body of the note. We will do this by demonstrating that, over most of the frequency range we are interested in (including the first stop-band frequency, where the inter-row spacing is about a half wavelength), the reflection coefficient of a single row of dielectric posts when the incident magnetic field is parallel to the posts is less than half the reflection coefficient of the single row of posts when the electric field is parallel to the posts. We will assume this to be sufficient evidence for the statement that, for almost all interesting frequencies, the reflection from several rows of posts will be a maximum when the incident electric field is parallel to the posts. Thus a rough bound on the reflection from a trestle can be obtained by assuming all the dielectric material to be concentrated into posts or sheets parallel to the electric field of the incident wave.

The proof, that an H-wave is reflected from a row of dielectric posts less than half as much as an E-wave, is rather lengthy, but it can be broken up into three shorter, logical parts.

First we will look at the H-wave scattering from a single dielectric post in the frequency range where equation (2.10) is valid. The result will be a field proportional to $\underline{\alpha}$, the normalized transverse static electric polarizability per unit length of the post. (i.e., the transverse electric dipole moment per unit length induced in the post, \underline{p} , is related to $\underline{\alpha}$ through $\underline{p} = \underline{\alpha}(\epsilon - \epsilon_0)A\underline{E}^{\text{ext}}$, where A is the cross-sectional area of the post and $\underline{E}^{\text{ext}}$ is the external electric field).

Next, we will show that R_H , the reflection coefficient when an H-wave is incident on a row of posts having a plane of symmetry perpendicular to the incident wave vector, is proportional to $\alpha_{yy}(kA/2d)(\epsilon_r - 1)E_y$, where E_y is the electric field at any post due to the incident wave and the scattering from all the other posts. This results in a relatively simple relationship between the reflection coefficient and α_{yy} , analogous to the representation of the reflection coefficient of an E-wave by the right hand side of equation (3.18).

Finally, we will derive bounds on α_{yy} . In fact we will show that α_{yy} is no greater than unity, and thus, for most frequencies of interest, we will be able to see simply that $|R_H| \leq \frac{1}{2}|R|$, where R is the reflection coefficient for an E-wave.

To discuss the scattering of an H-wave from a single dielectric post we will use the notation of figure 3, the incident magnetic field now being given by $\underline{H}^{inc} = \underline{e}_z H_o^{inc} e^{ikx}$. Invoking Green's theorem and the radiation condition, the total magnetic field can then be written (suppressing the subscript on H_z) in the form

$$H(\underline{\rho}) = H^{inc}(\underline{\rho}) + \int_C \left\{ H(\underline{\rho}') G_{n'}(\underline{\rho}, \underline{\rho}') - G(\underline{\rho}, \underline{\rho}') H_{n'}(\underline{\rho}') \right\} ds' \quad (A.1)$$

where

$$G(\underline{\rho}, \underline{\rho}') = \frac{i}{4} H_o^{(1)}(k|\underline{\rho} - \underline{\rho}'|) \quad (A.2)$$

$$= \frac{i}{4} J_o(k\rho') H_o^{(1)}(k\rho) + \frac{i}{2} \sum_{m=1}^{\infty} J_m(k\rho') H_m^{(1)}(k\rho) \cos m(\phi - \phi') \quad (A.3)$$

and, in equation (A.3), it is assumed that ρ is greater than ρ' .

The contribution of the first (zero-order) term on the right hand side of equation (A.3) to the integral on the right hand side of equation (A.1) may be calculated in a fairly straightforward manner when ρ is greater than any $|\underline{\rho}'|$ within the post. Denoting H outside the post by H_e and H inside the post by H_i , we have

$$\begin{aligned} I_o &\equiv \int_C \left\{ H_e(\underline{\rho}') \left[\frac{i}{4} J_o(k\rho') H_o^{(1)}(k\rho) \right]_{n'} - \left[\frac{i}{4} J_o(k\rho') H_o^{(1)}(k\rho) \right] H_{en'}(\underline{\rho}') \right\} ds' \\ &= \frac{i}{4} H_o^{(1)}(k\rho) \int_C \left[H_e(\underline{\rho}') \frac{\partial}{\partial n'} J_o(k\rho') - J_o(k\rho') \frac{\partial}{\partial n'} H_e(\underline{\rho}') \right] ds' \end{aligned}$$

$$\begin{aligned}
I_o &= \frac{i}{4} H_o^{(1)}(k\rho) \int_c \left\{ H_i(\underline{\rho}') \frac{\partial}{\partial n'} J_o(k\rho') - \frac{J_o(k\rho')}{\epsilon_r} \frac{\partial}{\partial n'} H_i(\underline{\rho}') \right\} ds' \\
&= \frac{i}{4} H_o^{(1)}(k\rho) \int_A \left\{ \nabla' \cdot \left\{ H_i(\underline{\rho}') \nabla' J_o(k\rho') - \frac{J_o(k\rho')}{\epsilon_r} \nabla H_i(\underline{\rho}') \right\} \right\} dS' \\
&= \frac{i}{4} H_o^{(1)}(k\rho) \int_A \left\{ \nabla' H_i(\underline{\rho}') \cdot \nabla' J_o(k\rho') \left(1 - \frac{1}{\epsilon_r}\right) + H_i(\underline{\rho}') \nabla'^2 J_o(k\rho') \right. \\
&\quad \left. - \frac{J_o(k\rho') \nabla'^2 H_i(\underline{\rho}')}{\epsilon_r} \right\} dS'
\end{aligned}$$

The second two terms of the integrand cancel, giving us

$$\begin{aligned}
I_o &= -\frac{ik}{4} H_o^{(1)}(k\rho) \frac{\epsilon_r - 1}{\epsilon_r} \int_A \frac{\partial H(\underline{\rho}')}{\partial \rho'} J_1(k\rho') \rho' d\rho' d\phi' \\
&= -\frac{ik}{4} H_o^{(1)}(k\rho) \frac{\epsilon_r - 1}{\epsilon_r} \int_A i\omega \epsilon E_\phi(\rho', \phi') J_1(k\rho') \rho' d\rho' d\phi'
\end{aligned}$$

or, since

$$\begin{aligned}
\int_0^{2\pi} E_\phi(\rho', \phi') \rho' d\phi' &= \int_{\text{around circle}} \underline{E} \cdot d\underline{s}' \\
&= \int_{\text{over circle}} \nabla \times \underline{E} \cdot d\underline{S}' \\
&= i\omega \mu_o \int_{\text{over circle}} H(\underline{\rho}') dS' \\
&= i\omega \mu_o H(\underline{O}) O(\pi\rho'^2),
\end{aligned}$$

we have

$$\begin{aligned}
I_0 &= \frac{k^3}{4} H_0^{(1)}(k\rho) \frac{\epsilon_r^{-1}}{\epsilon_r} H(0)0 \left\{ \int_A \frac{\rho J_1(k\rho) dS}{2} \right\} \\
&= H_0^{(1)}(k\rho) \frac{\epsilon_r^{-1}}{8\epsilon_r} H(0)0 [(ka)^4]
\end{aligned}$$

where "a" is some typical dimension of the cross section of the post.

The above pattern of calculation can be followed in determining the contributions of the other terms on the right hand side of equation (A.3) to the integral of equation (A.1). The result is that the terms of order two or higher contribute only to order $(ka)^4$ or higher, but that the first order term, which we will hereafter take as the dominant term at the frequencies we are interested in, contributes a term of order $(ka)^2$. In particular, if the x - y plane is a plane of post symmetry (which we will now assume; the proof carries through in general -- it just gets messier),

$$\begin{aligned}
I_1 &= -\frac{ck^2}{4} H_1^{(1)}(k\rho) \cos \phi \int_A (\epsilon - \epsilon_0) E_y(\underline{\rho}) dS \\
&= -\frac{ck^2}{4} H_1^{(1)}(k\rho) \cos \phi p_y,
\end{aligned} \tag{A.4}$$

where

$$\begin{aligned}
\underline{p} &\equiv \int_A \underline{p}(\underline{\rho}) dS \\
&\equiv \int_A (\epsilon - \epsilon_0) \underline{E}(\underline{\rho}) dS
\end{aligned} \tag{A.5}$$

is the transverse dipole moment per unit length induced in the dielectric post.

Making use of equation (A.4), we can now write the reflected H-wave from an infinite row of dielectric posts, when the incident wave vector is normal to the row, as

$$H^{\text{ref}}(x,y) = -\frac{ck^2 p_y}{4} \sum_{m=-\infty}^{\infty} \frac{x}{\sqrt{x^2 + (y-md)^2}} H_1^{(1)}\left(\frac{k\sqrt{x^2 + (y-md)^2}}{\lambda}\right) \quad (\text{A.6})$$

Invoking the Poisson summation formula, and differentiating with respect to x , the reflected E_y field can then be written in the form

$$E_y^{\text{ref}}(x,y) = \frac{1}{-i\omega\epsilon_0} \frac{\partial H}{\partial x} \\ = \frac{p_y k}{2\epsilon_0 d} \left\{ e^{-ikx} - 2 \sum_{m=1}^{\infty} \cos\left(\frac{2\pi my}{d}\right) e^{(2\pi x/d)\sqrt{m^2 - (d/\lambda)^2}} \right\}, \quad x < 0 \quad (\text{A.7})$$

thus

$$E_y^{\text{ref}}(x,y) \rightarrow \frac{p_y k}{2\epsilon_0 d} e^{-ikx} \quad \text{as } x \rightarrow -\infty, \quad (\text{A.8})$$

i.e.,

$$R_H = \frac{p_y k}{2\epsilon_0 d E_0^{\text{inc}}} \quad (\text{A.9})$$

We can now define a normalized dipole moment per unit length through

$$p_y \equiv (\epsilon - \epsilon_0) A \alpha_{yy} E_y$$

where E_y is the field at any particular dipole due to the incident wave and all the other dipoles (it is assumed that E_y is approximately uniform over the post), and thus we can rewrite equation (A.9) as

$$R_H = \frac{(\epsilon_r - 1)}{2} \frac{kA}{d} \alpha_{yy} \frac{E_y}{E_0^{\text{inc}}} \quad (\text{A.10})$$

But it can be shown that

$$\begin{aligned}
E_y &= E_o^{inc} + \frac{ick^2}{2\omega\epsilon_o} p_y \sum_{m=1}^{\infty} \frac{H_1^{(1)}(mkd)}{md} \\
&= E_o^{inc} + \frac{ikp_y}{2\epsilon_o d} S_2 \\
&= E_o^{inc} + \frac{i(\epsilon_r - 1)}{2} \frac{kA}{d} \alpha_{yy} E_y S_2 \\
&= \frac{E_o^{inc}}{1 - i(\epsilon_r - 1)(kA/d)\alpha_{yy}(S_2/2)}
\end{aligned} \tag{A.11}$$

where

$$S_2 \equiv \sum_{m=1}^{\infty} \frac{H_1^{(1)}(mkd)}{m} \tag{A.12}$$

Combining equations (A.10) and (A.11), we have

$$|R_H| = \left| \frac{(\epsilon_r - 1)(kA/d)(\alpha_{yy}/2)}{1 - i(\epsilon_r - 1)(kA/d)(\alpha_{yy}S_2/2)} \right| \tag{A.13}$$

This is to be compared with the other reflection coefficient, easily derived from the results of Section III,

$$|R| = \left| \frac{(\epsilon_r - 1)(kA/d)}{1 - i(\epsilon_r - 1)(kA/d)(kdS_1/2)} \right|$$

Thus we see that, except when kd is very close to those values where S_1 blows up (and S_1 does not blow up in the first, and most interesting, stop band if the inter-row spacing is greater than half the spacing between posts in a row, which is a weakened version of secondary assumption 4, Section I),

$$\left| \frac{R_H}{R} \right| \approx \alpha_{yy}/2 \quad (\text{A.14})$$

Before we go on to prove that α_{yy} is less than unity, it might be well to point out that S_2 can be transformed to a more easily computable sum by the following manipulations

$$\begin{aligned} \sum_{m=1}^{\infty} \frac{H_1^{(1)}(mx)}{m} &= \frac{1}{x} \sum_{m=1}^{\infty} \frac{xH_1^{(1)}(mx)}{m} \\ &= \frac{1}{x} \sum_{m=1}^{\infty} \left\{ -\frac{2i}{\pi m} + \int_0^x z H_0^{(1)}(mz) dz \right\} \\ &= -\frac{\pi i}{3x} + \frac{1}{x} \int_0^x z \left\{ -\frac{1}{2} + \frac{i}{\pi} \ln\left(\frac{\Gamma z}{4\pi}\right) + \frac{1}{2\pi z} \right. \\ &\quad \left. - 2i \sum_{m=1}^{\infty} \left[\frac{1}{\sqrt{(2\pi m)^2 - z^2}} - \frac{1}{2\pi m} \right] \right\} dz \\ &= -\frac{\pi i}{3x} + \frac{1}{2\pi} - \frac{x}{4} + \frac{ix}{\pi} \left[\ln\left(\frac{\Gamma x}{4\pi}\right) - \frac{1}{4} \right] \\ &\quad + \frac{2i}{x} \sum_{m=1}^{\infty} \left[2\pi m - \sqrt{(2\pi m)^2 - x^2} - \frac{x^2}{4\pi m} \right], \end{aligned}$$

but we will not determine any numerical values of S_2 in this note. The above transformation is merely for future reference, since it does not seem to be well known.

Now let us examine the normalized polarizability α_{yy} . We are dealing now with electrostatics, and so let us talk in terms of potentials. Let ϕ^{inc} be the potential of the incident electric field and ϕ be the potential of the total electric field. From the fact that

$$\int_A |\nabla(\phi - \phi^{inc})|^2 dS \geq 0,$$

where the integration is over the cross section of the post, we have

$$\int_A \nabla(\phi - \phi^{inc}) \cdot \nabla(\phi - \phi^{inc}) dS \geq 0$$

$$\int_A \nabla \cdot [(\phi - \phi^{inc}) \nabla(\phi - \phi^{inc})] dS \geq 0$$

$$\int_C (\phi - \phi^{inc}) (\phi - \phi^{inc})_n ds \geq 0$$

i.e.

$$\int_C \phi^{inc} \phi_n^{inc} + \int_C (\phi - \phi^{inc}) \phi_n \geq \int_C \phi \phi_n^{inc} \quad (A.15)$$

We will determine an appropriate expression for $(\phi - \phi^{inc})$ on the surface now. Denoting potentials in the exterior region by a superscript e and potentials in the interior region by a superscript i, we have, in the exterior region,

$$\phi^e = \phi^{inc} + \int_C [\phi^e G_{n'} - G \phi_n^e] ds'$$

and

$$0 = \int_c [\phi^i G_{n'} - G\phi_{n'}^i] ds'.$$

Subtracting these two equations, and using the boundary conditions

$$\phi^e = \phi^i$$

$$\phi_n^e = \epsilon_r \phi_n^i,$$

we can say that, in the exterior region, or on the surface,

$$\phi = \phi^{inc} - (\epsilon_r - 1) \int_c G\phi_n^i ds'. \quad (A.16)$$

Equation (A.16), when substituted into inequality (A.15), leads to

$$\int_c \phi^{inc} \phi_n^{inc} ds - (\epsilon_r - 1) \int_c \int_c \phi_n^{inc} G\phi_n^{inc} ds ds' \geq \int_c \phi \phi_n^{inc} ds. \quad (A.17)$$

But it is clear that the double integral in this inequality is a positive quantity since it can be thought of as being proportional (with a positive proportionality constant) to the total electrostatic energy corresponding to a surface charge distribution ϕ_n^{inc} . Thus

$$\int_c \phi \phi_n^{inc} ds \leq \int_c \phi^{inc} \phi_n^{inc} ds \quad (A.18)$$

Now let us specialize to the case where ϕ^{inc} is the potential of a uniform field in the y-direction (i.e., $\phi^{inc} = -E_o^{inc} y$). We then have

$$\begin{aligned} \int_c \phi^{inc} \phi_n^{inc} ds &= \int_A (\nabla \phi^{inc})^2 dS \\ &= (E_o^{inc})^2 A, \end{aligned} \quad (A.19)$$

while, from equation (A.5) and the definition of α_{yy} ,

$$\begin{aligned}
 \alpha_{yy} &= (AE_o^{inc})^{-1} \int_A E_y dS \\
 &= -(AE_o^{inc})^{-1} \int_A \frac{\partial \phi}{\partial y} dS \\
 &= (AE_o^{inc})^{-1} \int_C \phi (\underline{n} \cdot \underline{e}_y) ds \\
 &= \left(AE_o^{inc^2} \right)^{-1} \int_C \phi \phi_n^{inc} ds \tag{A.20}
 \end{aligned}$$

Thus, combining equations (A.19) and (A.20) with inequality (A.18), we have

$$\alpha_{yy} \leq 1, \tag{A.21}$$

and thus, from equation (A.14)

$$|R_H/R| \leq 1/2. \tag{A.22}$$

Inequality (A.22) is our reason for neglecting the H polarization in the main body of the text and our reason for saying that a rough bound on the reflection coefficient of a trestle structure can be obtained by assuming all dielectric material to be concentrated into the posts parallel to the incident electric field vector.

Before bringing this appendix to a close, there are two points of general interest about the immediately preceding electrostatic work.

The first point is that it was never essential to use the two dimensional character of our problem in proving inequality (A.21). The same inequality will hold for any diagonal element of the polarizability tensor of a three-

dimensional dielectric blob in the form

$$P_{xx} \leq (\epsilon_r - 1)V$$

where the induced dipole is given by $\underline{p} = \epsilon_0 \underline{p} \cdot \underline{E}_0^{inc}$.

The second point of interest is that, while working on the analytical proof of inequality (A.21), two integral equation formulations of the dielectric blob problem became evident. These two equations are for the determination of either the surface potential or the exterior normal derivative of surface potential (from either of which, the complete field distribution can be determined by quadrature) when a dielectric blob is immersed in an incident electric field. The two equations may be written in the forms

$$\phi(\underline{r}) = \frac{2}{\epsilon_r + 1} \phi^{inc}(\underline{r}) - 2 \frac{\epsilon_r - 1}{\epsilon_r + 1} \int_c G_n(\underline{r}, \underline{r}') \phi(\underline{r}') dS' \quad (A.22)$$

$$\phi_n(\underline{r}) = \frac{2\epsilon_r}{\epsilon_r + 1} \phi_n^{inc}(\underline{r}) - 2 \frac{\epsilon_r - 1}{\epsilon_r + 1} \int_c G_n(\underline{r}, \underline{r}') \phi_n(\underline{r}') dS'. \quad (A.23)$$

The first of these is well known (see, for example, [40], p. 75). The second is not so well known, but should be just as useful for numerical work. In fact, while equation (A.22) would seem to be appropriate for ϵ_r close to unity, equation (A.23) may be more appropriate as ϵ_r gets large.

Appendix B
A Matrix Inversion

In Section IV we found it necessary to solve the set of equations

$$x_n + c \sum_{m=1}^N e^{ikD|n-m|} x_m = y_n \quad 1 \leq n \leq N. \quad (B.1)$$

This appendix gives the method of solving the above set.

To start with, let us look at the above set in the range $1 < n < N$.

Then we can write any of the remaining equations in any of the three following forms

$$x_n + c \sum_{m=1}^n e^{ikD(n-m)} x_m + c \sum_{m=n+1}^N e^{ikD(m-n)} x_m = y_n \quad (B.2)$$

$$x_{n+1} + ce^{ikD} \sum_{m=1}^n e^{ikD(n-m)} x_m + ce^{-ikD} \sum_{m=n+1}^N e^{ikD(m-n)} x_m = y_{n+1} \quad (B.3)$$

$$x_{n-1} + ce^{-ikD} \sum_{m=1}^n e^{ikD(n-m)} x_m + ce^{-ikD} \sum_{m=n+1}^N e^{ikD(m-n)} x_m + 2ic \sin kD x_n = y_{n-1} \quad (B.4)$$

Equations (B.3) and (B.4) come about by the replacements $n \rightarrow n \pm 1$ in equation (B.2), while adjusting the limits on the sums to be the same as those in equation (B.2) by adding or subtracting appropriate terms. Now, if we add equations (B.3) and (B.4) and from the sum subtract $2 \cos kD$ times equation (B.2), we obtain

$$x_{n+1} - 2(\cos kD - ic \sin kD)x_n + x_{n-1} = y_{n+1} - 2 \cos kD y_n + y_{n-1}. \quad (B.5)$$

This equation, as we said above, is true in the range $1 < n < N$. Let us see what we have to do to make it true for $1 \leq n \leq N$. By looking at equation (B.5) for $n = 1$ and $n = N$, it can be seen that (B.5) can be assumed to be true in the total range of n if we define

$$y_0 \equiv e^{ikD} y_1 \quad (\text{B.6})$$

$$y_{N+1} \equiv e^{ikD} y_N \quad (\text{B.7})$$

and we set

$$x_0 = e^{ikD} x_1 \quad (\text{B.8})$$

$$x_{N+1} = e^{ikD} x_N \quad (\text{B.9})$$

Thus equations (B.1) are equivalent to the difference equation (B.5) with the boundary conditions (B.8) and (B.9) and with the subsidiary definitions (B.6) and (B.7). Let us find the solution to equations (B.5) by finding a "Green's function" defined by

$$G_{n+1,m} - 2 \cos \theta G_{n,m} + G_{n-1,m} = \delta_{n,m} \quad (\text{B.10})$$

along with boundary conditions equivalent to (B.8) and (B.9) and auxiliary definitions equivalent to (B.6) and (B.7). In equation (B.10), $\delta_{n,m}$ is the Kronecker delta function, and we have written

$$\cos \theta = \cos kD - ic \sin kD. \quad (\text{B.11})$$

Once $G_{n,m}$ is found we can clearly write the solution for x_n in the form

$$x_n = \sum_{m=1}^N G_{n,m} (y_{m+1} - 2 \cos kD y_m + y_{m-1}) \quad (\text{B.12})$$

or, equivalently,

$$x_n = \sum_{m=1}^N (G_{n,m-1} - 2 \cos kD G_{n,m} + G_{n,m+1}) y_m - G_{n,0} y_1 + G_{n,1} y_0 - G_{n,N+1} y_N + G_{n,N} y_{N+1} \quad (\text{B.13})$$

Thus, assuming for the moment the symmetry of $G_{n,m}$ (i.e., that $G_{n,m} = G_{m,n}$), it follows from equation (B.13), by using equations (B.6) through (B.11), that

$$x_n = y_n - 2ic \sin kD \sum_{m=1}^N G_{n,m} y_m. \quad (\text{B.14})$$

Equations (B.12) and (B.14) are two alternative representations of the solution, x_n , of equation (B.1). It remains to determine an explicit formula for $G_{n,m}$. From this explicit formula, the symmetry that we required above will be obvious.

The solution of equation (B.10) for either $n > m$ or $n < m$ must be a linear combination of the two homogeneous difference equation solutions. Let us look at the case $n < m$. Then it follows from direct substitution in the homogeneous difference equation that

$$G_{n,m} = A \sin n\theta + B \cos n\theta \quad n < m \quad (\text{B.15})$$

is a solution, where A and B are to be determined. Boundary condition (B.8) implies

$$A \sin \theta + B \cos \theta = e^{-ikD} B$$

and thus

$$G_{n,m} = \frac{B}{\sin \theta} \{ \sin \theta \cos n\theta - \cos \theta \sin n\theta + e^{-ikD} \sin n\theta \} \quad n < m$$

$$= \frac{B}{\sin \theta} \{ e^{-ikD} \sin n\theta - \sin(n-1)\theta \} \quad n < m. \quad (\text{B.16})$$

Similarly

$$G_{n,m} = \frac{C}{\sin \theta} \{e^{-ikD} \sin(N+1-n) - \sin(N-n)\}, \quad n > m, \quad (\text{B.17})$$

or, in order to assure equality of the two expressions when $n = m$, we may write

$$G_{n,m} = K \frac{e^{-ikD} \sin n\theta - \sin(n-1)\theta}{e^{-ikD} \sin m\theta - \sin(m-1)\theta} \quad n < m \quad (\text{B.18})$$

$$G_{n,m} = K \frac{e^{-ikD} \sin(N+1-n)\theta - \sin(N-n)\theta}{e^{-ikD} \sin(N+1-m)\theta - \sin(N-m)\theta} \quad n > m \quad (\text{B.19})$$

In order to determine K , we substitute the above expressions in equation (B.10) for $n = m$ and find

$$1 - 2K \cos \theta = K \frac{e^{-ikD} \sin(N-m)\theta - \sin(N-p-1)\theta}{e^{-ikD} \sin(N+1-p)\theta - \sin(N-p)\theta} + K \frac{e^{-ikD} \sin(m-1)\theta - \sin(m-2)\theta}{e^{-ikD} \sin m\theta - \sin(m-1)\theta} \quad (\text{B.20})$$

When K is determined from equation (B.20) and substituted back in equations (B.18) and (B.19) the result, after algebraic simplification is

$$G_{n,m} = \frac{[e^{-ikD} \sin(N+1-m)\theta - \sin(N-m)\theta][e^{-ikD} \sin n\theta - \sin(n-1)\theta]}{\sin \theta e^{-ikD} [2 \sin N\theta - e^{ikD} \sin(N-1)\theta - e^{-ikD} \sin(N+1)\theta]} \quad n \leq m \quad (\text{B.21})$$

$$G_{n,m} = \frac{[e^{-ikD} \sin(N+1-n)\theta - \sin(N-n)\theta][e^{-ikD} \sin m\theta - \sin(m-1)\theta]}{\sin \theta e^{-ikD} [2 \sin N\theta - e^{ikD} \sin(N-1)\theta - e^{-ikD} \sin(N+1)\theta]} \quad n \geq m \quad (\text{B.22})$$

Thus the solution of equations (B.1) is completed.

References

- [1] Carl E. Baum, "General Principles for the Design of Atlas I and II, Part I: Atlas: Electromagnetic Design Considerations for Horizontal Version," Sensor and Simulation Notes, Note 143, January 1972.
- [2] Carl E. Baum, "General Principles for the Design of Atlas I and II, Part II: Atlas: Electromagnetic Design Considerations for Vertical Version," Sensor and Simulation Notes, Note 144, January 1972.
- [3] Carl E. Baum, "General Principles for the Design of Atlas I and II, Part III: Additional Considerations for the Design of the Terminations," Sensor and Simulation Notes, Note 145, March 1972.
- [4] Carl E. Baum, "General Principles for the Design of Atlas I and II, Part IV: Additional Considerations for the Design of Pulser Arrays," Sensor and Simulation Notes, Note 146, March 1972.
- [5] Carl E. Baum, "EMP Simulators for Various Types of Nuclear EMP Environments: An Interim Categorization," Sensor and Simulation Notes, Note 151, July 1972.
- [6] Philip M. Morse and Herman Feshbach, Methods of Theoretical Physics, — (McGraw-Hill, New York, 1953).
- [7] Jack H. Richmond, "Scattering by a dielectric cylinder of arbitrary cross section shape," IEEE trans. Antennas Propagat., Vol. AP-13, No. 3, May 1965, pp. 334-341.
- [8] J. Van Bladel, "Low-frequency scattering by cylindrical bodies," Appl. Sci. Res., Section B, Vol. 10, 1964, pp. 195-202.
- [9] K. Mei and J. Van Bladel, "Low-frequency scattering by rectangular cylinders," IEEE trans. Antennas Propagat., Vol. AP-11, No. 1, Jan. 1963, pp. 52-56.
- [10] H. C. Van de Hulst, Light Scattering by Small Particles, (Wiley, New York, 1957).
- [11] M. Kerker, D. D. Cooke, and J. M. Carlin, "Light scattering from infinite cylinders, the dielectric-needle limit," Jour. Optical Soc. America, Vol. 60, No. 9, Sept. 1970, pp. 1236-1239.
- [12] D. S. Jones, The Theory of Electromagnetism, (Macmillan, New York, 1964).
- [13] Milton Abramowitz and Irene A. Stegun, Editors, Handbook of Mathematical Functions, National Bureau of Standards, AMS-55, 1964.

- [14] Donald R. Wilton and Raj Mittra, "A new numerical approach to the calculation of electromagnetic scattering properties of two-dimensional bodies of arbitrary cross section," IEEE trans. Antennas Propagat., Vol. AP-20, No. 3, May 1972, pp. 310-317.
- [15] A. W. Maue, "Zur Formulierung eines allgemeinen Beugungsproblems durch eine Integralgleichung," Z. Physik, Vol. 126, Aug. 1949, pp. 601-618.
- [16] Claus Müller, "Über die Beugung elektromagnetischer Schwingungen an endlichen homogenen Körpern," Math., Annalen, Vol. 123, 1951, pp. 345-378.
- [17] Claus Müller, Grundprobleme der Mathematischen Theorie Elektromagnetischer Schwingungen, (Springer-Verlag, 1957).
- [18] F. K. Oshiro, K. M. Mitzner, S. S. Locus et al, "Calculation of radar cross section, Part II, Analytical Report," Technical report AFAL-TR-70-21, part II, April 1970.
- [19] R. W. Latham and K. S. H. Lee, "Theory of Inductive Shielding," Interaction Notes, Note 12, March 1968.
- [20] Carl E. Baum, "Admittance sheets for terminating high-frequency transmission lines," Sensor and Simulation Notes, Note 53, April 1968.
- [21] R. W. Latham and K. S. H. Lee, "Termination of two parallel semi-infinite plates by a matched admittance sheet," Sensor and Simulation Notes, Note 68, January 1969.
- [22] James R. Wait, "Reflection from a wire grid parallel to a conducting plane," Canad. Jour. Phys., Vol. 32, No. 9, Sept. 1954, pp. 571-579.
- [23] L. Infeld, V. G. Smith and W. Z. Chen, "On some series of Bessel functions," Jour. Math. and Phys., Vol. 26, 1947, pp. 22-28.
- [24] Horace Lamb, "On the reflection and transmission of electric waves by a metallic grating," Proc. London Math. Soc., Vol. 29, 1898, pp. 523-544.
- [25] W. von Ignatowsky, "Theory of the grating," Ann. Physik, Vol. 44, 1914, pp. 369-436.
- [26] W. von Wessel, "On the passage of electromagnetic waves through a wire grid," Hochfrequenztechnik, Vol. 54, No. 1, Jan. 1939, pp. 62-69.
- [27] G. G. MacFarlane, "Surface impedance of an infinite wire grid at oblique angles of incidence, Jour. IEE, Vol. 93, No. 12, Dec. 1946, pp. 1523-1527.

- [28] Richard Honerjager, "On the diffraction of electromagnetic waves by a wire grid," *Ann. Physik*, Vol. 4, No. 1, Jan 1948, pp. 25-35.
- [29] Edward A. Lewis and Joseph P. Casey, Jr., "Electromagnetic reflection and transmission by gratings of resistive wires," *Jour. App. Phys.*, Vol. 23, No. 9, June 1952, pp. 605-608.
- [30] Willice E. Groves, "Transmission of electromagnetic waves through pairs of parallel wire grids," *Jour. App. Phys.*, Vol. 24, No. 7, July 1953, pp. 845-854.
- [31] James R. Wait, "Reflection at arbitrary incidence from a parallel wire grid," *Appl. Sci. Res.*, Vol. B4, March 1954, pp. 393-400.
- [32] James R. Wait, "Effective impedance of a wire grid parallel to the earth's surface," *IRE trans. Antennas Propagat.*, Vol. AP-10, No. 5, Sept. 1962, pp. 538-542.
- [33] M. I. Kontorovich, V. Yu. Petrun'kin, N. A. Yesepkina, and M. I. Astrakhan, "The coefficient of reflection of a plane electromagnetic wave from a plane wire mesh," *Rad. Eng. and Electron. Phys.*, 1962, pp. 222-231.
- [34] M. I. Kontorovich, "Averaged boundary conditions at the surface of a grating with square mesh," *Rad. Eng. and Electron. Phys.*, Vol. 8, No. 9, 1963, pp. 1446-1454.
- [35] M. I. Astrakhan, "Averaged boundary conditions on the surface of a lattice with rectangular cells," *Rad. Eng. and Electron. Phys.*, Vol. 9, No. 8, 1964, pp. 1239-1241.
- [36] M. I. Kontorovich, M. I. Astrakhan, and M. N. Spirina, "Slowing down of electromagnetic waves by wire meshes," *Rad. Eng. and Electron. Phys.*, Vol. 9, No. 8, 1964, pp. 1242-1245.
- [37] M. I. Astrakhan, "Reflecting and screening properties of plane wire grids," *Radio Engineering (U.S.S.R.)*, Vol. 23, No. 1, 1968, pp. 76-83.
- [38] Gerrit J. van den Broek and Jacob van der Vooren, "On the reflection properties of periodically supported metallic wire gratings with rectangular mesh showing small sag," *IEEE trans. Antennas Propagat.*, Vol. AP-19, No. 1, Jan. 1971, pp. 109-112.
- [39] D. A. Hill and J. R. Wait, "Scattering of a transient plane wave by a periodic grating," *Radio Science*, Vol. 6, No. 11, Nov. 1971, pp. 1003-1009.
- [40] J. Van Bladel, Electromagnetic Fields, (McGraw-Hill, New York, 1964).